Environmental Research 197 (2021) 111083

Contents lists available at ScienceDirect

Environmental Research

journal homepage: www.elsevier.com/locate/envres

Review article

An integrated approach for assessing the *in vitro* and *in vivo* redox-related effects of nanomaterials

Periklis Vardakas [a], Zoi Skaperda [a], Fotios Tekos [a], Aikaterini-Flora Trompeta [b], Aristidis Tsatsakis [c], Constantinos A. Charitidis [b], Demetrios Kouretas [a,*]

[a] *Department of Biochemistry-Biotechnology, University of Thessaly, 41500, Larissa, Greece*

[b] *Research Lab of Advanced, Composite, Nano-Materials and Nanotechnology, School of Chemical Engineering, National Technical University of Athens, 9 Heroon Polytechniou St. Zografos, 157 80, Athens, Greece*

[c] *Laboratory of Toxicology Science and Research, Medical School, University of Crete, 71003, Heraklion, Crete, Greece*

A R T I C L E I N F O

Keywords:
Nanomaterials
Redox biology
Oxidative stress
Toxicology
Environmental imprint
Human health

A B S T R A C T

Over the last few decades, nanotechnology has risen to the forefront of both the research and industrial interest, resulting in the manufacture and utilization of various nanomaterials, as well as in their integration into a wide range of fields. However, the consequent elevated exposure to such materials raises serious concerns regarding their effects on human health and safety. Existing scientific data indicate that the induction of oxidative stress, through the excessive generation of Reactive Oxygen Species (ROS), might be the principal mechanism of exerting their toxicity. Meanwhile, a number of nanomaterials exhibit antioxidant properties, either intrinsic or resulting from their functionalization with conventional antioxidants. Considering that their redox properties are implicated in the manifestation of their biological effects, we propose an integrated approach for the assessment of the redox-related activities of nanomaterials at three biological levels (*in vitro*-cell free systems, cell cultures, *in vivo*). Towards this direction, a battery of translational biomarkers is recommended, and a series of reliable protocols are presented in detail. The aim of the present approach is to acquire a better understanding with respect to the biological actions of nanomaterials in the interrelated fields of Redox Biology and Toxicology.

1. Introduction

Nanotechnology, as defined by US National Nanotechnology Initiative, refers to “a science, engineering, and technology conducted at the nanoscale (1–100 nm), where unique phenomena enable novel applications in a wide range of fields, from chemistry, physics and biology, to medicine, engineering and electronics”. The interest in this field emerged in the 1980s, and since the early 2000s has achieved tremendous progress with the discovery or manufacture of a vast number of nanomaterials (NMs), accompanied by increased claims regarding their properties, behaviors and potential utilizations (Read et al., 2014). Nowadays there are several pieces of legislation in Europe and USA, with specific references to NMs, however, a universally agreed definition does not yet exist (Boverhof et al., 2015). In consonance with the definition adopted by European Commission, a NM is “a natural, incidental or manufactured material containing particles, in an unbound state or as an aggregate or as an agglomerate and where, for 50% or more of the particles in the number size distribution, one or more external dimensions is in the size range 1–100 nm”. The physicochemical characteristics of NMs, which can be selectively modified, have given them prominence due to their enhanced performance in comparison with their bulk counterparts (Jeevanandam et al., 2018). Consequently, they are widely used in diverse fields, such as constructions (Gajanan and Tijare, 2018), electronics (Mishra et al., 2017; Bondavalli et al., 2019), environmental protection (Kausar, 2019) and consumer products (Contado, 2015), providing quality upgrade and novel features, while recently the scientific interest has been focused on their potential applications in biomedical research and drug delivery systems (Kuskov et al., 2017; Luss et al., 2018; Taghizadehghalehjoughi et al., 2018; Radu et al., 2019; Berdiaki et al., 2020).

Even though NMs are offering multiple technical advantages, their increased manufacturing and their industrial applications are followed by an increased risk of human and environmental exposure, thus raising serious concerns about human safety and health. It is worth noting that human exposure results from different sources (environment, workplace, commercial products) and by different routes (inhalation, trans-

* Corresponding author. University of Thessaly, Department of Biochemistry and Biotechnology, Viopolis, Mezourlo, Larissa, 41500. Greece.
E-mail address: dkouret@uth.gr (D. Kouretas).

https://doi.org/10.1016/j.envres.2021.111083
Received 9 February 2021; Received in revised form 22 March 2021; Accepted 22 March 2021
Available online 26 March 2021
0013-9351/

dermal, ingestion) (Kuhlbusch et al., 2018). In view of the fact that powders are risk factors in the workplace, and most of the engineered NMs are in the form of dry powders, exposure through inhalation is a parameter of great concern regarding the workers in such facilities (Pietroiusti et al., 2018; Oberbek et al., 2019). On the contrary, the exposure of general population occurs mainly through skin contact or ingestion, during the use of nanotechnology products (Sharma et al., 2012). Products consumed or applied directly to the skin may have greater exposure potential, whereas exposure to NMs that are incorporated into relatively durable matrices is expected to be minimal, indicating that the exposure is also influenced by the nature of the product (Thomas et al., 2009).

With respect to potential routes of NMs exposure, inhalation has definitely received the most attention, and is extensively considered as the main route of concern. Lungs are the primary organs targeted by inhaled NMs (Landsiedel et al., 2014). During acute exposure, pulmonary toxicity arises predominantly in the form of an inflammatory response, whereas chronic exposure to such materials constitutes a risk factor for pulmonary fibrosis (Saifi et al., 2018b). The oral entry of NMs is considered as a completely different case, since the prevailing gastrointestinal conditions are not encountered within the other routes of exposure, and they are also capable of affecting NMs toxicity profile. To be more specific, the acidic pH of stomach and the elevated ionic strength of gastrointestinal fluids are expected to significantly affect the physicochemical properties of the ingested NM, conceivably leading to various toxic products (Bouwmeester, van der Zande and Jepson, 2018). On the other hand, their trans-dermal entry remains a controversial issue, and generally raises the least concerns regarding potential toxicity, as current studies indicate that the entry through skin penetration is highly limited (Watkinson et al., 2013; Staroń et al., 2020). Based on the fact that the physicochemical properties of NMs are implicated in their ability to penetrate the skin barrier (Nafisi and Maibach, 2018), some of them reside in the outer layer of skin, inducing local adverse effects, whereas others are capable of reaching the deeper layers, thus entering to systemic circulation (Larese Filon et al., 2015).

The environmental entry of NMs is expected to be either direct, through the use of nanotechnology products, or indirect via the disposal of industrial waste (Klaper, 2020). After the release of NMs in the main environmental matrices (air, soil, water), their fate is not only dependent on the impact of their physicochemical properties, but also on their interplay with other environmental contaminants (Kabir et al., 2018). Additionally, the general inability to detect NMs following their release into the environment further prolongs the duration of their effects and hence intensifies their consequences. Aquatic ecosystems represent the primary pools of NMs environmental entry, as well as the main sources of their spread to other environmental resources (Turan et al., 2019). In this light, several nanotoxicity studies have been carried out primarily on marine microorganisms (Balmuri et al., 2017; Pikula et al., 2018, 2020; Kirichenko et al., 2019), because of their abundance and high sensitivity to environmental contaminants, and secondarily on aquatic animals (Raman et al., 2016), ultimately indicating the aquatic toxicity induced by various NMs. Besides their effects on the corresponding ecosystems, as well as on the growth and survival of microorganisms, plants and animals (Bakshi, 2020), the contamination of environmental matrices might also affect human health through direct and daily contact with them, thus creating a vicious cycle (Fig. 1).

The physicochemical characteristics of NMs are not only responsible for their technical advantages, but also for their adverse effects related with toxic biological outcomes in humans (Viswanath and Kim, 2017). Size, surface chemistry and morphology are key factors from a toxicological aspect, while shape, aspect ratio, chemical composition, solubility, agglomeration state and crystal structure are also critical parameters for the manifestation of NMs effects (Gatoo et al., 2014; Allegri et al., 2016). Standardized and validated characterization methods for measuring physicochemical properties of NMs seem at this point a prerequisite, in order to correlate properties with health and safety risks (Gao and Lowry, 2018; Xiarchos et al., 2020). Moreover, the toxicity profile of NMs is significantly affected by the dose level and the exposure time (Jeevanandam et al., 2018). Fig. 2 summarizes the physicochemical characteristics of NMs, that are the main contributors for their toxic effects (Navya and Daima, 2016).

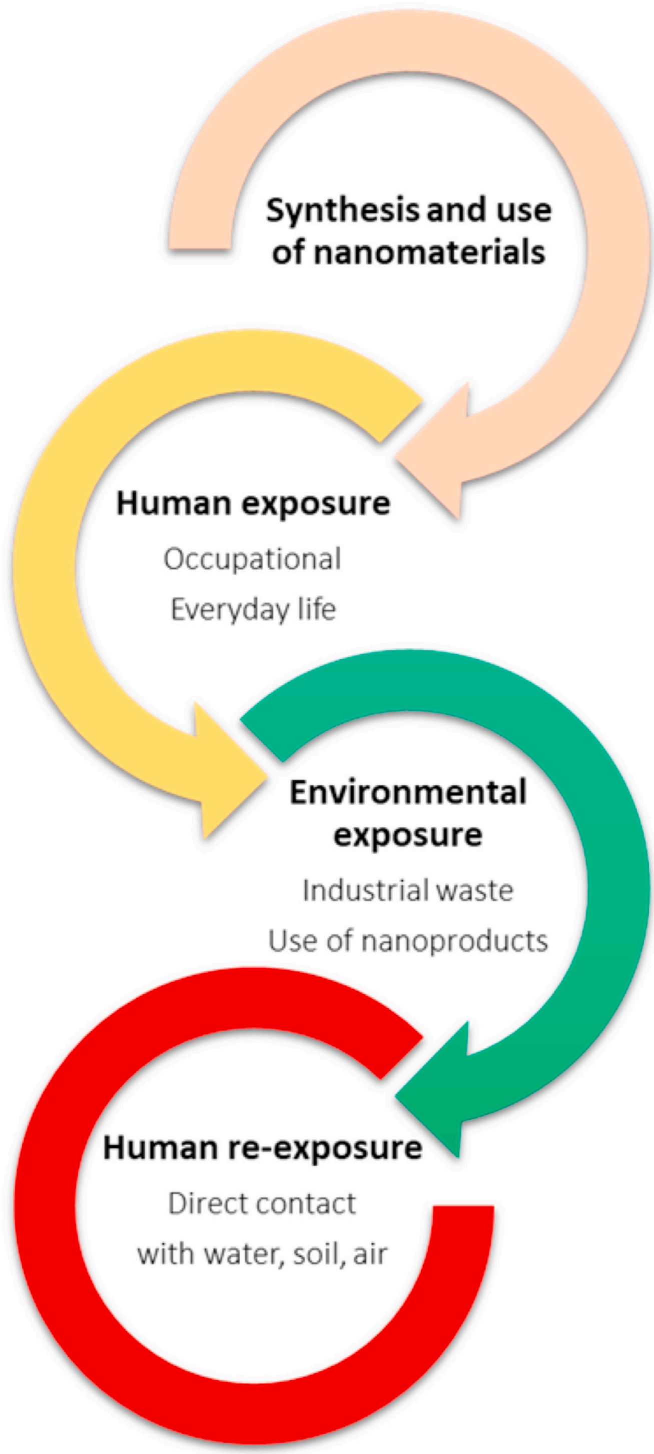

Fig. 1. Human and environmental exposure to nanomaterials.

Scientific evidence indicates that the induction of oxidative stress via ROS generation is emerging as one of the main mechanisms of NMs to exert adverse effects (Sharifi et al., 2012; Bostan et al., 2016; Saifi et al., 2018; Mendoza and Brown, 2019). Noteworthy, NMs are able to induce the generation of reactive species either directly or secondarily through

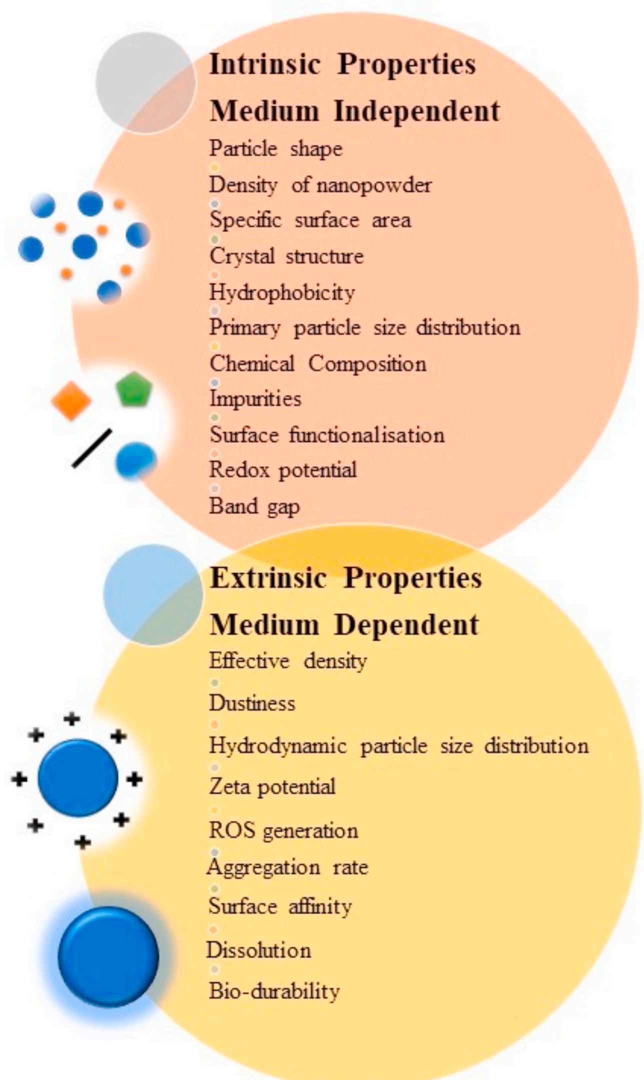

Fig. 2. Intrinsic and extrinsic properties of NMs affecting their toxicity.

the immune response provoked by their presence (Pietroiusti et al., 2014). Specifically, the direct interaction of nanoparticles with electrons released from mitochondria or mitochondria per se can cause an increase of superoxide radical ($O_2^{\bullet-}$) levels (Dayem et al., 2017). Moreover, nanoparticles consisting of transition metals or metal oxides are involved in the generation of the highly reactive hydroxyl radicals ($OH^{\bullet}$), capable of initiating the lipid peroxidation process (Mylonas and Kouretas, 1999) through Haber-Weiss and Fenton reactions (Fu et al., 2014). It should also not be neglected that NMs can activate NADPH oxidase, a part of phagocytes physiological defense system, thus providing an additional mechanism of ROS generation (Engin et al., 2017; Mendoza and Brown, 2019).

Oxidative stress is present in numerous pathophysiological conditions, such as cancer, neurodegenerative, cardiovascular and respiratory diseases (Sosa et al., 2013; Csányi and Miller, 2014; van Raamsdonk et al., 2017; Hecker, 2018; Tekos et al., 2020), and its detrimental effects can be compensated by antioxidants (Pisoschi and Pop, 2015). Nevertheless, clinical trials have indicated the inability of known antioxidants to prevent the progression of ROS-related diseases, whereas at high doses they also exert adverse effects. Contrariwise, the use of nanoparticles may potentially overcome such limitations, due to their ability to control the biodistribution and specificity of conventional antioxidants (Ferreira et al., 2018). Paradoxically, in addition to antioxidant-functionalized nanoparticles, several types of NMs, including carbon, metal and metal oxides nanoparticles exhibit intrinsic antioxidant activities based on their surface properties (Fenoglio et al., 2006; Dellinger et al., 2013; Dhall and Self, 2018; Valgimigli et al., 2018). For instance, cerium oxide nanoparticles exert antioxidant activities both *in vitro* and *in vivo*, owing to the regenerative capacity of their surface, as a result of the redox-cycling between Ce^{3+} and Ce^{4+} ionic states (Dhall and Self, 2018). Consequently, NMs represent one of the most promising research fields for improved antioxidants, and they have emerged as an alternative strategy for scavenging reactive species *in vivo* (Liu and Shi, 2019). In this regard, the evaluation of the potential antioxidant properties of NMs is a field of particular interest.

NMs have been extensively used in the last decades, leading progressively to the intensification of exposure rates. Notwithstanding that the scientific publications have increased significantly over the years, the majority of the published studies focuses on the manufacture and development of new NMs, while in contrast a minority of them deals with their engineering and biological effects in a combinatorial manner (Coricovac et al., 2017; Pinzaru et al., 2018). As a result, there is insufficient understanding of their unique toxicological properties, as well as of their long-term effects on human health (Sharifi et al., 2012). Generally, the effects of NMs on biological systems are attributed to and influenced by their unique redox properties either antioxidant or pro-oxidant (Sims et al., 2017). Actually, in some cases the same NM can exert double-edged effects. For instance, several metal and metal oxide nanoparticles mimic the activity of the antioxidant enzyme catalase at neutral or basic pH values, whereas at acidic pH values a prooxidant effect is observed (Valgimigli et al., 2018). Therefore, the comprehensive evaluation of the redox-related effects of NMs will contribute significantly to the understanding of their complex nature and their effects on biological entities.

To the best of our knowledge, so far, a holistic approach for the evaluation of NMs impact in the field of Redox Biology does not exist. Based on the above, the aim of the present publication is to propose an integrated approach for the assessment of NMs redox-related effects at three biological levels (*in vitro*-cell free systems, cell cultures, *in vivo*), using a battery of translational redox biomarkers (Veskoukis et al., 2019). Besides the detailed presentation of the approach, we also attempt to provide specific protocols, the most reliable in our opinion, for the determination of the proposed redox biomarkers. Since Redox Biology and Toxicology are two research fields regularly interconnected, the evaluation of NMs effects in all three of the above mentioned levels is essential for the purpose of holistically unravelling their biological actions.

2. Assessment of NMs effects in *in vitro*-cell free systems

The use of appropriate *in vitro* biomarkers represents the first step to assess the redox-related activities of NMs. At this level, the effects of NMs are evaluated via *in vitro* biomarkers classified in three main categories. The first two categories include biomarkers for evaluating the potential antioxidant properties of NMs, including their antiradical and reducing capacity, as well as their ability to prevent from free radical-induced DNA damage. The biomarkers involved in these categories have been successfully employed for the determination of the antioxidant properties of plant and food components (Apostolou et al., 2013; Priftis et al., 2015; Mikropoulou et al., 2018; Kouka et al., 2019), dietary supplements (Kerasioti et al., 2014) and biological samples (Grundler et al., 2020), while their use has also been extended to the study of NMs (Zare et al., 2018; Genc, 2020). More specifically, the potential antiradical capacity of NMs is evaluated spectrophotometrically by examining their ability to scavenge the commercially available free radicals 2, 2′-azino-bis(3-ethylbenzothiazoline-6-sulphonic acid) ($ABTS^{\bullet+}$) and 2, 2-diphenyl-1-picrylhydrazyl ($DPPH^{\bullet}$), and the naturally produced free radicals superoxide ($O_2^{\bullet-}$) and hydroxyl ($OH^{\bullet}$). Furthermore, for the purpose of evaluating NMs reducing capacity, the reducing power assay is performed. To this end, we propose a series of reliable protocols, presented in detail within the section 2.1. Additionally, the ability of NMs to prevent from the free radical induced-DNA damage is evaluated through electrophoresis on an agarose gel by examining their ability to inhibit DNA lesions. Towards this end, the peroxyl ($ROO^\bullet$) radical-induced plasmid DNA strand cleavage assay is proposed. The protocol is presented in the section 2.2.

On the contrary, the third category of biomarkers investigates the potential genotoxic effects of NMs on a low-complexity biological system by assessing their ability to induce mutagenesis in bacteria cells. Based on data so far, there is no evidence that NMs induce different types of genotoxicity than the ones induced by common chemical compounds, and therefore the evaluation of their potential genotoxic properties is a key element in NMs risk assessment (Haase and Luch, 2016). For this purpose, various *in vitro* assays can be performed, including Ames test, chromosomal aberration test, micronucleus assay, comet assay and mammalian cell gene mutation assays (Ng et al., 2010; Elespuru et al., 2018). However, Ames test provides a rapid and relatively simple process for evaluating a compounds ability to induce mutagenesis (Zeiger, 2019), and it is widely applied for assessing NMs genotoxic effects (Yoshida et al., 2009; Balasubramanyam et al., 2010; Li et al., 2012; Woodruff et al., 2012; Du et al., 2019). The genotoxic effects of NMs are evaluated by examining their ability to induce mutagenesis in *Salmonella typhimurium* cells (section 2.3). A NM capable of inducing mutations that allow the bacteria to revert back to their histidine synthesis ability is deemed to be a mutagen.

Concerning the translational potency, there are several parameters that limit the clinical significance of *in vitro* biomarkers. The biological systems are characterized by different levels of complexity, and thus lack of correlation between *in vitro* and *in vivo* settings is a common phenomenon. Focusing on NMs study, a major limitation arising from *in vitro* assays is that the exposure and dispersion methods do not adequately simulate the *in vivo* exposure (Park et al., 2009). Furthermore, the physicochemical characteristics of NMs enable them to interact rapidly *in vivo* with endogenous biomolecules, mainly proteins, forming protein bio-coronas that significantly alter their initial effects (Neagu et al., 2017; Meng et al., 2018). Despite the limitations of extrapolating safe conclusions regarding the *in vivo* settings, the selection and use of appropriate *in vitro* biomarkers still provide important information.

2.1. Antiradical and reducing capacity

2.1.1. $ABTS^{\bullet+}$ radical scavenging assay

2.1.1.1. Selected assay. Concerning the $ABTS^{\bullet+}$ assay, we propose the method of Cano et al. (2000) with some modifications.

2.1.1.2. Principle of the assay. The generation of $ABTS^{\bullet+}$ radicals results from the oxidation of 2,2′-azino-bis-(3-ethyl-benzthiazoline-sulphonic acid) diammonium salt (ABTS) by hydrogen peroxide (H_2O_2) via the catalytic activity of horseradish peroxidase (HRP). However, in the presence of an antioxidant compound, the generated free radicals are neutralized, and the green-colored radical solution is discolored, thus leading to an absorbance decrease at 730 nm.

2.1.1.3. Protocol. In test tubes, 400 μl dH_2O, 500 μl of an ABTS solution (1 mM), 50 μl of H_2O_2 (30 μM) and 50 μl of horseradish peroxidase (HRP) (6 μM) in phosphate-buffered saline (50 mM, pH = 7.5) are added. The samples are vortexed and incubated for 45 min in the dark at room temperature (RT) for the generation of $ABTS^{\bullet+}$ radicals. Then, 50 μl of the test NM, properly dispersed at various concentrations, is added to the mixture, and subsequently the absorbance is measured at 730 nm. In each experiment, a blank consisting of 450 μl dH_2O, 500 μl of the radical solution and 50 μl of H_2O_2, and a control comprising 400 μl dH_2O, 500 μl of the radical solution, 50 μl of H_2O_2 and 50 μl of HRP are also prepared. To calculate the radical scavenging capacity percentage (% RSC) of the test NM, the following equation is used:

$$\%\ ABTS^{\cdot+}RSC = \left[\left(Abs_{control} - Abs_{sample}\right) / Abs_{control}\right] \times 100$$

$Abs_{control}$ and Abs_{sample} stand for the absorbance of the control and the test NM, respectively. The radical scavenging efficacy of different NMs is compared by estimating an IC50 value. Specifically, IC50 refers to the concentration of the test NM required for the 50% inhibition of the respective free radical. The lower the IC50 value, the greater the radical inhibition capacity of the test NM.

2.1.2. $DPPH^\bullet$ radical scavenging assay

2.1.2.1. Selected assay. Regarding the $DPPH^\bullet$ assay, we propose the method of Brand-Williams et al. (1995) with some slight modifications.

2.1.2.2. Principle of the assay. In the presence of an antioxidant compound, the commercially available free radical $DPPH^\bullet$ is converted to the corresponding hydrazine, resulting in an absorbance decrease at 517 nm.

2.1.2.3. Protocol. In detail, 50 μl of the test NM, properly dispersed at different concentrations, is added in test tubes, followed by the addition of 900 μl of methanol (MeOH) and 50 μl of a $DPPH^\bullet$ solution (2 mM) in MeOH. Furthermore, 1 ml of MeOH is used as a blank and 950 μl of MeOH and 50 μl of $DPPH^\bullet$ solution are used as a control. The samples are vortexed, incubated for 20 min in the dark at RT and, then, the absorbance is measured at 517 nm. The % RSC of the test NM is calculated through the same equation as the one described for the $ABTS^{\bullet+}$ assay. Additionally, an IC50 value should be estimated for comparing the radical scavenging efficiency of different NMs.

2.1.3. Superoxide ($O_2^{\bullet-}$) radical scavenging assay

2.1.3.1. Selected assay. With respect to the scavenging activity of the superoxide ion radicals, we propose the method of Gülçin et al. (2004) with some minor modifications.

2.1.3.2. Principle of the assay. Superoxide radicals are derived from the phenazine methosulfate-nicotinamide adenine dinucleotide-nitroblue tetrazolium (PMS-NADH-NBT) generating system. In the presence of an antioxidant compound, the superoxide anion is scavenged, and consequently an absorbance decrease is observed at 560 nm.

2.1.3.3. Protocol. According to the assay, 50 μl of the test NM, properly dispersed at different concentrations, is mixed with 625 μl of Tris-HCl buffer (16 mM, pH = 8.0), 125 μl of NBT (300 μM) and 125 μl of NADH (468 μM) in test tubes. The reaction is initiated following the addition of 125 μl of PMS (60 μM) into the sample. In each experiment, a blank comprising 800 μl of Tris-HCl buffer, 125 μl of NBT and 125 μl of NADH, and a control containing 50 μl dH_2O, 625 μl of Tris-HCl buffer, 125 μl of NBT, 125 μl of NADH and 125 μl of PMS are also prepared. The samples are vortexed and incubated for 5 min in the dark at RT. After that, the absorbance is measured at 560 nm. The % RSC of the test NM is calculated using the equation that has been mentioned formerly for the $ABTS^{\bullet+}$ assay. Furthermore, an IC50 value should be estimated in order to compare the radical scavenging activity among different NMs.

2.1.4. Hydroxyl ($OH^\bullet$) radical scavenging assay

2.1.4.1. Selected assay. For the purpose of determining the scavenging activity of hydroxyl radicals, we propose a previously described method with slight modifications (Chung et al., 1997).

2.1.4.2. Principle of the assay. Hydroxyl radicals, that are produced by Fenton reaction, oxidize 2-deoxyribose, which is further decomposed into malondialdehyde (MDA). The reaction of MDA with thiobarbituric acid (TBA) leads to the production of a colored complex, absorbing maximal at 520 nm. In the presence of an antioxidant compound, hydroxyl radicals are scavenged, and an absorbance decrease at 520 nm is observed.

2.1.4.3. Protocol. In particular, 50 μl of the test NM, properly dispersed at various concentrations, is added to 225 μl of phosphate buffer (0.2 M, pH = 7.4), 75 μl of 2-deoxyribose (5 mM), 75 μl of a $FeSO_4$-EDTA solution (10 mM), 75 μl of H_2O_2 (10 mM) and 250 μl of dH_2O. In each experiment, a blank consisting of 225 μl of phosphate buffer, 75 μl of 2-deoxyribose, 75 μl of $FeSO_4$-EDTA solution and 375 μl of dH_2O, as well as a control containing 225 μl of phosphate buffer, 75 μl of 2-deoxyribose, 75 μl of $FeSO_4$-EDTA solution, 75 μl of H_2O_2 and 300 μl dH_2O are also prepared. The samples are vortexed and incubated at 37 °C for 1 h. After incubation, 375 μl of 2.8% trichloroacetic acid (TCA) and 375 μl of 1% TBA in NaOH (50 mM) are added, and the samples are transferred in a water bath for 10 min at 95 °C. Subsequently, the samples are placed on ice for 5 min and centrifuged (3000 rpm, 5 min, 25 °C). Eventually, the absorbance is monitored at 520 nm. To calculate the % RSC of the test NM, the equation that has been previously described for $ABTS^{\bullet+}$ assay is used. For the purpose of comparing the radical scavenging activity of different NMs, an IC50 value should be estimated.

2.1.5. Reducing power assay

2.1.5.1. Selected assay. To evaluate the reducing power of the test NM we propose a slightly modified method of Yen and Duh (1993).

2.1.5.2. Principle of the assay. In the presence of an antioxidant compound, ferrous (Fe^{+3}) ions are reduced to ferric (Fe^{+2}) ions, and their reaction with the added iron chloride leads to the production of a colored complex, with maximal absorbance at 700 nm.

2.1.5.3. Protocol. In test tubes, 50 μl of the test NM, properly dispersed at various concentrations, is added to 200 μl of phosphate buffer (0.2 M, pH = 6.6) and 250 μl of potassium ferricyanide (1% w/v) in dH_2O. It has to be noted that 500 μl of phosphate buffer is prepared as a blank, and 250 μl of phosphate buffer mixed with 250 μl of potassium ferricyanide are prepared as a control. The samples are vortexed and incubated for 20 min at 50 °C. Thereafter, the samples are cooled for 5 min, and 250 μl of 10% TCA is added, followed by centrifugation (3000 rpm, 10 min, 25 °C). Then, 700 μl of the supernatant is transferred in new test tubes, and 250 μl of dH_2O and 50 μl of ferric chloride (0.1%) are added. The samples are vortexed and incubated for 10 min in the dark at RT. Following incubation, the increase of absorbance is monitored at 700 nm. An AU0.5 value, standing for the NM concentration at which an OD_{700} of 0.5 is achieved, is calculated for the purpose of comparing the reducing power of different NMs.

2.2. Protection against the free radical-induced DNA damage

2.2.1. Peroxyl radical ($ROO^{\bullet}$)-induced plasmid DNA strand cleavage

2.2.1.1. Selected assay. The method is performed as described previously (Priftis et al., 2017; Kouka et al., 2019).

2.2.1.2. Principle of the assay. The conformational changes of plasmid DNA affect its mobility when electrophoresed on an agarose gel. In particular, under the influence of peroxyl radicals, which are generated from the thermal decomposition of 2,2′-azobis(2-amidinopropane hydrochloride) (AAPH), the supercoiled conformation of plasmid DNA is converted to the open circular, after a single-strand break. The open circular conformation runs slower on the gel than the supercoiled one.

2.2.1.3. Protocol. Regarding the assay, in a final volume of 10 μl the test NM, properly dispersed at various concentrations, is mixed with 3.2 μg of plasmid DNA (pBluescript SK+), sterilized phosphate buffered saline (PBS) and AAPH (95 mM) in PBS. The samples are vortexed and incubated for 45 min at 37 °C. In each experiment, a negative control containing plasmid DNA and PBS, and a positive control containing plasmid DNA, PBS and AAPH are also used. Additionally, plasmid DNA is treated with the highest concentration of the test NM for the purpose of evaluating its effects on the supercoiled conformation. Following incubation, the reaction is stopped by adding 3 μl of a loading buffer (bromophenol blue 0.25% + 30% glycerol), and the samples are electrophoresed on a 0.8% agarose gel at 80 V for 1 h. Subsequently, the gel is transferred in a solution containing 12,5 μl of ethidium bromide (10 μg/ml) and 250 ml of dH_2O in order to be stained for 30 min, and thereafter it is washed with 250 ml of dH_2O for an additional time of 15 min. Eventually, the gel is exposed to UV, the image is captured and the results are analyzed using an image analysis quantification software. To calculate the percentage of the protective activity of the test NM, the following equation is used:

$$\% \text{ Inhibition} = [(S - So) / (S_{control} - S_o)] \times 100$$

Regarding the equation, the factor S represents the percentage of the supercoiled plasmid DNA in the test samples, while S_o stands for the percentage of the supercoiled plasmid DNA in the positive control. Furthermore, $S_{control}$ represents the percentage of the supercoiled DNA in the negative control. To compare the protective activity of different NMs against the $ROO^{\bullet}$-induced DNA damage, an IC50 value should be estimated.

2.3. Mutagenicity

2.3.1. Ames test

The mutagenic properties of NMs are evaluated through the Ames test (Maron and Ames, 1983). Regarding the principle of the assay, histidine auxotroph *Salmonella typhimurium* strains are grown in plates, in the presence or absence (control) of a mutagen under investigation. When an external source of histidine is lacking, the bacteria cells are unable to form colonies, while in contrast the cells reverting to their initial histidine independence have regained this ability. The addition of a mutagen leads to an increase of the number of colonies per plate, typically in a dose-dependent manner. Concerning the experimental procedure, for a 30 ml inoculation of autoclaved Oxoid nutrient broth no. 2, 700 μl of the *Salmonella typhimurium* TA102 (MolTox) bacterial culture are used. The cultures are vibrated (100 rpm), placed in the dark at a laboratory incubator at 37 °C, and the absorbance is frequently monitored at 540 nm. An OD_{540} ranging between 0.1 and 0.2 is expected, since it indicates that the bacteria cells have reached a density of $1–2 \times 10^9$ colony forming units (CFU/ml). Afterward, 2 ml of top agar, 100 μl of the bacterial culture and 50 μl of each NM, properly dispersed at various concentrations, are added in sterile tubes and vortexed. Subsequently, the content of the sterile tubes is poured onto plates, which have been covered previously by glucose minimal agar, and the plates are incubated for 48 h at 37 °C. It has to be noted that a plate without the test NM is used as a control. Lastly, the colonies reverted to their histidine independence are counted. To determine the mutagenic properties of the test NM, the number of spontaneous revertants on the control plate is subtracted from the number of revertants on the plates with the test NM.

3. Assessment of NMs effects in cell cultures

Notwithstanding that the cell cultures are widely considered as an *in vitro* condition, in essence, they comprise an intermediate level between *in vitro* and *in vivo* settings, hence providing a useful *in-vivo* like system for the evaluation of the redox-related effects of NMs. The selection of the cell line depends on the potential route by which the NM of interest enters the body. Since NMs are capable of exhibiting cytotoxicity at the portal entry, the cells in the epithelium of the respective organs, as well as the cells of the innate immune system are ideal for examining the toxic effects of NMs (Mrakovcic et al., 2013). Macrophages are widely preferred in nanotoxicity studies, as they represent the first responders following NMs exposure, implicated in their recognition, internalization and clearance (Drasler et al., 2017; Figueiredo Borgognoni et al., 2018). In order to obtain relevant information regarding NMs-induced inhalation toxicity, various tissues of the respiratory system are used, including cells derived from the epithelium of human airway and alveoli, as well as alveolar macrophages (Bakand and Hayes, 2016). Regarding ingestion exposure, the epithelial cells of intestine are regularly used in nanotoxicity studies, since intestine represents one of the main organs of NMs entry in the body (Drasler et al., 2017). Notwithstanding that skin constitutes a potential route of exposure, recent studies indicate that the trans-dermal entry is limited (Staroń et al., 2020). However, for the purpose of acquiring useful information on the toxicity induced via this route, keratinocytes and fibroblasts are mainly used. Finally, given the fact that NMs have been recruited as potential allies in the research of cancer therapy, various tumor cell lines are also used for evaluating the toxic, yet beneficial in the present case, effects of NMs (Sukhanova et al., 2018).

The duration of exposure to NMs differs significantly among the various publications, depending on the selected exposure scenario (e.g. industrial accident, occupational exposure, everyday life exposure). Typically, the cell-based assays are used to simulate scenarios that correspond to a daily exposure rather than a chronic one. However, a sub-chronic scenario might be simulated via repeated exposures to the NM of interest, provided that the cellular system remains sustainable for such a period of time (Drasler et al., 2017). Regarding the simulation of an everyday-life condition, a 24 h exposure to low concentrations of the test NM might provide an insight into the exposure of the general population. Meanwhile, shorter time intervals (30 min, 1 h, 3 h) have already been used for the purpose of simulating an occupational condition, such as an industrial accident (Kyriakidou et al., 2020).

The development of novel but also relevant for human studies *in vitro* systems is a primary objective in the field of Toxicology in order to extrapolate safer conclusions regarding the effects on human health. Although the conventional 2D monolayer cell cultures are a useful tool, they do not adequately reflect the prevailing *in vivo* conditions (Edmondson et al., 2014). Specifically, the cell-cell interactions and the interactions between cells and the extracellular matrix, implicated into key processes of cell growth and behavior, are not taken into account (Da Rocha et al., 2014). Undeniably, the *ex vivo* organ cultures can counteract the aforementioned restrictions, also allowing the maintenance of the physiological functions of the respective organ. However, the acquisition of the tissue sample and the short viability of those cell cultures are still limiting factors (Chia et al., 2015; Al-Lamki et al., 2017). In this regard, a panel of 3D cell culture systems has emerged as a powerful alternative to properly simulate the architecture and the microenvironment of the tissue of interest (Al-Lamki et al., 2017). It should be emphasized that 3D cell cultures are characterized by substantial heterogeneity in terms of the cellular components (primary cells or established cell lines) (Koledova, 2017), the way of culturing (monocultures or co-cultures) (Ravi et al., 2015) and after all the technology used for the cell culture development (e.g. spheroids, scaffolds, organoids, organ-on-chip) (Fang and Eglen, 2017). The aforementioned methods have also been incorporated as a valid, *in vivo*-like model into the testing of NMs toxicity (Lee et al., 2009; Chia et al., 2015; Wu et al., 2017).

In the present approach, following the selection of the preferred cell line and exposure scenario, the redox-related effects of NMs are evaluated by investigating their cytotoxicity, their effects on redox biomarkers and on the expression of important antioxidant genes. The proposed experimental procedure has been carried out formerly for the evaluation of the redox-related properties in endothelial cells (Goutzourelas et al., 2015; Kerasioti et al., 2020).

A wide range of cell viability assays has been used in the literature for the evaluation of NMs cytotoxicity, with more or less reliability, including tetrazolium salt-based assays, resazurin reduction, trypan blue exclusion assay, neutral red uptake assay and lactate dehydrogenase assay (Nogueira et al., 2014; Kyriakidou et al., 2020). Depending on the test NM, the appropriate cell viability assay should be chosen in order to avoid possible limitations and misleading conclusions (Wörle-Knirsch et al., 2006; Wang et al., 2011; Breznan et al., 2015; Forest et al., 2015). Even though the trypan blue exclusion assay was proposed about a century ago, it remains the most widely used method for determining cell viability, and it is regularly employed in NMs study to overcome such limitations (Hoskins et al., 2012; Piccinini et al., 2017). Hence, we propose the use of the specific method in the section 3.2.

Whereupon, the cells are exposed to the selected subtoxic concentrations, and a network of redox biomarkers, adequately reflecting the cellular redox state, are determined either by flow cytometry or spectrophotometry. In particular, the intracellular levels of reduced glutathione (GSH) and ROS are determined by flow cytometry, using the fluorescent dyes mercury orange and 2′,7′-Dichlorofluorescein diacetate (DCF-DA), respectively. GSH is the most important and abundant hydrophilic antioxidant, protecting cells from the detrimental effects of electrophiles (Aquilano et al., 2014), whereas ROS are implicated in the oxidative damage of various biomolecules (Mylonas and Kouretas, 1999; Kunwar, A., Priyadarsini, 2011), and their excessive generation induces oxidative stress. Furthermore, total antioxidant capacity (TAC), thiobarbituric acid reactive substances (TBARS) and protein carbonyls are determined by spectrophotometry. Briefly, TAC refers to the antioxidant capacity of the components present in a biological sample (Soumya and Vani, 2015). On the contrary, TBARS and protein carbonyls are products of lipid peroxidation and protein carbonylation, respectively, and they represent biomarkers of severe oxidative damage. Actually, the TBARS method is well established for monitoring lipid peroxidation (Sochor et al., 2012), while the heavy carbonylated proteins are widely regarded as a biomarker of oxidative stress (Gonos et al., 2018). The selected protocols are described in detail within the section 3.3.

Previous studies have reported that NMs are able to induce the activation of nuclear factor erythroid 2-related factor 2 (Nrf2), leading to an elevated expression of enzymes associated with cellular defense mechanisms (Hussain et al., 2014; Lai et al., 2015; Liu et al., 2017). The primary transcription factor Nrf2 coordinates the regulation of oxidant and antioxidant responses, subsequent to a redox altering stimuli, such as xenobiotics and pathological conditions (Ma, 2013; Veskoukis et al., 2020). Under basal conditions, Nrf2 activity is suppressed by its cytoplasmic interaction with Kelch-like ECH-associated protein 1 (Keap1), that functions as an adaptor for ubiquitination factors, leading to Nrf2 rapid degradation by proteasomes (Kobayashi et al., 2006). Contrariwise, under oxidative stress conditions, Nrf2 is disassociated from its complex with Keap1, stabilized and translocated to the nucleus in order to activate the expression of antioxidant response elements (AREs)-dependent genes (Panieri et al., 2020). These genes encode a wide variety of important antioxidant and detoxifying enzymes, constituting the majority of intracellular defense mechanisms, and as a result, the analysis of this gene network provides a first insight regarding the mechanism of action of NMs. In this light, we propose quantitative Real-Time PCR for the purpose of quantifying the expression of superoxide dismutase (SOD), catalase (CAT), glutathione peroxidase (GPx), glutathione reductase (GR), thioredoxin (TRX), glutamate-cysteine ligase catalytic subunit (GCLC), NAD(P)H quinone oxidoreductase (NQO1), heme oxygenase-1 (HO-1) and Nrf2 (section 3.4). Additionally, as the prediction of protein levels from mRNA levels generally lacks of precision (Maiväli, 2015), Western blot analysis is also proposed for determining the cellular localization of Nrf2 and for detecting the possible differences in the expression levels of its target genes (section 3.4).

3.1. Cell treatment

The cells are seeded in 25 cm^2 culture flasks with the appropriate complete medium and incubated for 24 h at 37 °C in 5% CO_2 and 80–95% humidity in order to reach about 80% confluency. Then, the complete medium is discarded, the test NM, properly dispersed at various concentrations, is added to serum-free medium and the cells are incubated for a time period corresponding to the selected exposure scenario. The cells that have not been treated with the test NM are considered as control group. Thereafter, the serum-free medium is discarded, the cells are trypsinized and centrifuged (1500 rpm, 5 min, 5 °C). Following the disposal of the supernatant, the cells are washed with PBS and centrifuged (1500 rpm, 5 min, 5 °C) one more time. After the second centrifugation, the supernatant is discarded, and the cell pellet is collected.

3.2. Cytotoxicity

3.2.1. Trypan blue exclusion assay

The assay is performed as reported previously by Stagos et al. (2014). The principle of the assay is dependent on the ability of live cells to exclude stains, through their intact cell membranes, while in contrast dead cells do not possess the same ability (Strober, 2015). Regarding the assay, after exposure to the test NM the serum-free medium is discarded and the cells are trypsinized and centrifuged (1500 rpm, 5 min, 5 °C). Then, the supernatant is discarded and the cell pellet is resuspended in serum-free medium or PBS at 1×10^6 cells/ml. Eventually, equal volumes (1:1) of the cell suspension and the trypan blue stain (0.4% w/v) are mixed and unstained and blue-stained cells, representing viable and non-viable cells, respectively, are counted using either a hemocytometer and a phase contrast microscope or an automated cell counter.

3.3. Determination of redox biomarkers

3.3.1. Assessment of GSH and ROS levels by flow cytometry

The determination of GSH and ROS levels by flow cytometry is performed as described previously by Kouka et al. (2017). Regarding the assay, a mercury orange stock solution (400 μM) is prepared in acetone and stored at 4 °C, whereas a DCF-DA stock solution (400 μM) is prepared in methanol on the day of the experiment. Following the preparation of the dye stock solutions, the cell pellet (see section 3.1) is resuspended in PBS at 1×10^6 cells/ml. Afterward, 150 μl of the cell suspension is transferred into flow cytometry tubes and incubated with either 15 μl of mercury orange (40 μM) or 15 μl of DCF-DA (10 μM) for 30 min in the dark at 37 °C. After incubation, the cells are washed with 250 μl of PBS, centrifuged (1500 rpm, 5 min, 5 °C) and resuspended in 250 μl of PBS. Eventually, the cell suspension is subjected to flow cytometric analysis. The excitation and emission wavelengths for ROS are at 488 and 530 nm and for GSH at 488 and 580 nm. The size of the cells and their internal complexity are measured by the forward and right-angle light scattering, respectively. The analysis is performed on 10000 cells per sample, at a flow rate of 1000 events/sec, and the intensity of the fluorescence is measured on a logarithmic scale.

3.3.2. Assessment of TAC, TBARS and protein carbonyls by spectrophotometry

The cell pellet (see section 3.1) is resuspended with whole cell lysis buffer [Tris (20 mM), NaCl (150 mM), 1% Nonidet P40 (NP-40), pH = 7.5], containing protease inhibitors. The cells are incubated for 20 min on ice and centrifuged (16250 g, 20 min, 4 °C). The supernatant is collected and used for the determination of the redox biomarkers.

Prior to the assays, the total protein concentration of the cell lysate is estimated through the Bradford assay (Bradford, 1976) and used for the normalization of the redox biomarkers. To estimate the total protein concentration of the cell lysate, a standard curve is required, using various concentrations of a known protein as standards, where bovine serum albumin (BSA) is one of the most common.

3.3.2.1. Total antioxidant capacity (TAC)

3.3.2.1.1. Selected assay. To determine the cellular TAC levels, we propose the protocol of Janaszewska and Bartosz (2002).

3.3.2.1.2. Principle of the assay. TAC levels are determined using the free radical $DPPH^{\bullet}$. In the presence of an antioxidant molecule, acting as a hydrogen donor, $DPPH^{\bullet}$ is reduced to the corresponding hydrazine, and its reduction is evaluated spectrophotometrically through the decrease of absorption at 520 nm.

3.3.2.1.3. Protocol. In detail, an amount of cell lysate, containing at least 30 μg of protein, and an equal amount of cell lysis buffer for the control, is added to 450 μl of phosphate buffer (10 mM, pH = 7.4) and 500 μl of $DPPH^{\bullet}$ solution (0.1 mM) in MeOH. The samples are vortexed and incubated for 1 h in the dark at RT. Thereafter, the samples are centrifuged (15000 g, 3 min, 25 °C), and the absorbance is monitored at 520 nm. The levels of TAC are calculated as the mmol of $DPPH^{\bullet}$ reduced to the corresponding hydrazine by the antioxidant molecules of cell lysate, and the results are presented as mmol DPPH/mg protein.

3.3.2.2. Thiobarbituric acid reactive substances (TBARS)

3.3.2.2.1. Selected assay. For the determination of TBARS levels, we propose the method of Keles et al. (2001) with slight modifications.

3.3.2.2.2. Principle of the assay. MDA, a byproduct of lipid peroxidation that exerts strong mutagenic effects (Ayala et al., 2014), is quantified through the reaction with TBA to produce TBARS. TBARS are expressed as equivalents of MDA, forming a 1:2 complex with TBA, which can be measured spectrophotometrically at 530 nm.

3.3.2.2.3. Protocol. An amount of cell lysate, containing at least 100 μg of protein, and an equal amount of cell lysis buffer for the control, is added to falcon tubes and mixed with 500 ml of 35% TCA and 500 ml of a Tris-HCl buffer (200 mM, pH = 7.4). The samples are vortexed and incubated for 10 min at RT. Subsequently, 1 ml of a solution consisting of Na_2SO_4 (2 M) and TBA (55 mM) is added, and the samples are transferred in a water bath for 45 min at 95 °C. Following incubation, the samples are cooled for 5 min, and 1 ml of 70% TCA is added to the mixture. Eventually, the samples are centrifuged (11200 g, 3 min, 25 °C), and the absorbance is monitored at 530 nm. The molar extinction coefficient of MDA (156000 mol/l) is used for the determination of TBARS concentration, and the results are presented as μmol TBARS/mg protein.

3.3.2.3. Protein carbonyls

3.3.2.3.1. Selected assay. Concerning protein carbonyl levels, we propose the method of Patsoukis et al. (2004) with slight modifications.

3.3.2.3.2. Principle of the assay. The derivatization of the carbonyl group with 2,4-dinitrophenylhydrazine (DNPH) results in the production of 2,4-dinitrophenyl (DNP), which absorbs maximal at 375 nm.

3.3.2.3.3. Protocol. According to the assay, an amount of cell lysate, containing at least 100 μg of protein, is mixed with an equal amount of 20% TCA, the samples are vortexed and incubated in an ice bath for 15 min. Following incubation, the samples are centrifuged (15000 g, 5 min, 4 °C), and the supernatant is discarded. Afterward, 500 μl of a DNPH solution (10 mM) in HCl (2.5 N) or 500 μl of 2.5N HCl is added to the samples or controls, respectively (each sample has its own control). The samples are incubated for 1 h in the dark at RT and vortexed intermittently every 15 min. Thereafter, the samples are centrifuged (15000 g, 5 min, 4 °C). The disposal of the supernatant is followed by the addition of 1 ml of 10% TCA, a vigorous vortex and a centrifugation (15000 g, 5 min, 4 °C). Then, the supernatant is discarded, 1 ml of a mixture containing ethanol-ethyl acetate (1:1 v/v) is added, and the samples are vortexed and centrifuged (15000 g, 5 min, 4 °C). After discarding the supernatant, the aforementioned step is repeated once more.

Thereupon, 1 ml of urea (5 M, pH = 2.3) is added to the samples, and the tubes are vortexed and placed at an incubator for 15 min at 37 °C. Lastly, a centrifugation (15000 g, 3 min, 4 °C) is required, and the absorbance is monitored at 375 nm. To determine protein carbonyls concentration, the millimolar extinction coefficient of DNPH (22 l/mol/cm) is used, and the results are expressed as nmol protein carbonyls/mg protein.

3.4. NMs effects on the expression of Nrf2 and its target genes

3.4.1. Quantitative Real-Time PCR (qRT-PCR) of Nrf2 and its target genes

The assay is performed as reported formerly by Stagos et al. (2018). Initially, the RNA is extracted from the cell pellet (see section 3.1) using an RNA isolation kit. After RNA extraction, a quantification and a validation of its purity are required, and the whole process is carried out through the measurement of OD_{260}/OD_{280} ratio. A value greater than 1.8 indicates lack of protein contamination. The second step includes the digestion of the extracted RNA with DNase. For this purpose, ~10 μg of RNA is mixed with 10 μl of DNase (1 U/μl), 4 μl of a PCR buffer (10x) and sterilized dH_2O in a final volume of 40 μl. The samples are placed in a laboratory incubator for 30 min at 37 °C, and the reaction is stopped with the addition of 4 μl of a stop solution. Thereafter, the samples are incubated for 10 min at 65 °C. In the next step, the reverse transcription of DNA-free RNA is performed in 20 μl reactions in order to obtain cDNA. In particular, ~3 μg of the pure DNA is mixed with 1 μl of oligo (dT) (12–18 primers), 1 μl of deoxynucleotide triphosphates (dNTPs) and sterilized dH_2O. The samples are incubated for 5 min at 65 °C and transferred on ice for an additional time of 5 min. Afterward, 4 μl of a PCR buffer (5x) and 2 μl of dithiothreitol (DTT) are added, and the samples are incubated for 2 min at 42 °C. Following incubation, 1 μl of reverse transcriptase is added to the mixture, and the samples are incubated initially for 50 min at 42 °C and then for 15 min at 70 °C. The last step is the amplification of the selected genes (NFE2L2, HMOX1, NQO1, GCLC, CAT, SOD1, GSR, GPX, TXN and GAPDH). On that note, 25 ng of cDNA is mixed with 0.25 μM of each primer, SYBR® Select Master Mix (2X, applied biosystems, USA) and ROX Low (50 nM) in a final volume of 10 μl. The appropriate primers can be selected based on bibliography. To amplify the cDNAs, the following thermocycling conditions have been selected: 3 min at 95 °C, 45 cycles of 15 s at 95 °C and 30 s at 53 °C, followed by 30 s at 72 °C. Finally, the specificity of the products is checked using a melting curve from 53 °C to 95 °C. The expression of mRNA levels in each sample is normalized to glyceraldehyde 3-phosphate dehydrogenase (GAPDH) mRNA levels.

3.4.2. Western blot analysis of Nrf2 and its target genes

Prior to the assay, the whole cell lysate, as well as the cytosolic and nuclear lysates are prepared. To prepare the whole cell lysate, the cell pellet (see section 3.1) is resuspended in RIPA buffer [Tris-HCl (50 mM), NaCl (150 mM), 0.25% SDS, 0.25% sodium deoxycholate, EDTA (1 mM), pH = 8.0], containing protease inhibitors. Then, the sample is centrifuged (16250 g, 20 min, 4 °C), and the supernatant is collected. For the preparation of the cytosolic and nuclear lysates, the cell pellet is resuspended in cytosolic lysis buffer [HEPES-KOH (10 mM, pH = 7.9), $MgCl_2$ (1.5 mM), KCl (10 mM), dithiothreitol (DTT) (0.5 mM), 0.5% NP-40], containing protease inhibitors. The samples are transferred on ice for 20 min and centrifuged (16250 g, 5 min, 4 °C). The supernatant is collected (cytosolic lysate), and the formed pellet is resuspended in nuclear lysis buffer [HEPES-KOH (10 mM, pH = 7.9), 25% glycerol, NaCl (420 mM), $MgCl_2$ (1.5 mM), EDTA (0.2 mM), DTT (0.5 mM), 0.5% Triton X-100)], containing protease inhibitors. Afterward, the samples are transferred on ice for 20 min, sonicated periodically for 30 s and centrifuged (16250 g, 15 min, 4 °C). The amount of protein in the whole, cytosolic and nuclear lysates is estimated through the Bradford assay.

Thereafter, immunoblot analysis is performed as reported formerly (Kerasioti et al., 2016) in order to determine the expression levels of Nrf2, SOD, CAT, HO-1 and GCS. In particular, to determine the levels of SOD, CAT and HO-1, an amount of whole cell lysate that contains 50 μg of protein is used. Moreover, for the determination of the cytosolic levels of Nrf2 and GCS, an amount of cytosolic lysate that contains 30–50 μg of protein is used. Finally, the levels of nuclear Nrf2 are determined using the nuclear lysate. The cell lysates are separated by SDS-PAGE electrophoresis on 8% polyacrylamide gel at 150 V for 45–60 min. Subsequently, the proteins are transferred on polyvinylidene difluoride membranes (PVDF), which are blocked overnight at 4 °C with 5% non-fat milk in Tris-buffered saline with Tween-20 (TBST) [Tris (13 mM), NaCl (150 mM), 0.2% Tween-20, pH = 7.5]. Afterward, the membranes are probed with primary antibodies [rabbit anti-human/mouse Nrf2 (1:2000), goat anti-human/mouse SOD-1 (1:1600), goat anti-human/mouse CAT (1:1400), goat anti-human/mouse HO-1 (1:1400), rabbit anti-human/mouse GCS (1:1600)] at RT for 1 h. Whereupon, it follows the incubation of membranes with HRP secondary antibodies [anti-goat (1:3000) or anti-rabbit (1:5000)] for 30 min at RT. It has to be noted that GAPDH is used as an internal control for the cytosolic lysate, whereas the proliferating cell nuclear antigen (PCNA) serves the same purpose for the nuclear lysate. Lastly, an image analysis quantification software is used for the quantification of protein levels via the optical density of protein bands.

4. Assessment of NMs effects *in vivo*

The *in vivo* study is a prerequisite for investigating the biological effects of continuous exposure to NMs, due to the fact that the complexity of *in vivo* systems provides unique mechanisms of biodistribution, metabolism, excretion and immune responses (Smith et al., 2016). However, the toxicokinetic studies performed to date are disproportionate to the number of the engineered NMs, and therefore our knowledge of the procedures that follow after their entry in the body is limited (Piperigkou et al., 2016). Humans are daily exposed to complex mixtures of environmental contaminants, and the widespread use of NMs definitely classifies them among their main components (Tsiaoussis et al., 2019). In this light, specific strategies have been developed to assess the effect of low doses of mixtures, containing routinely encountered xenobiotics, over long periods of time, thus simulating the real-life exposure scenario (Tsatsakis et al., 2016; Tsatsakis et al., 2017). Although the short-term exposure to low doses of such mixtures may not exhibit immediate toxic effects, and is even capable of inducing strong adaptive mechanisms, the long-term exposure may potentially lead to toxicity (Docea et al., 2018; Fountoucidou et al., 2019). Taking this into consideration, the effects of acute and chronic exposure to low doses of NMs should be evaluated in order to determine their impact on human health.

Even though studies on human populations are the most direct evidence of NMs biological outcome, most of the available information originates from studies carried out in cell cultures or more directly in experimental animals. Besides the ethical issues, several parameters restrict the conduct of studies on human beings, among them the relatively small sample size and the lack of industries exclusively occupied with the manufacture of nanotechnology products (Liou et al., 2015). It is worth noting that the existing studies are mainly focused on employees in such facilities rather than the general public, because of their daily exposure through NMs handling. From early findings, redox parameters seem to be particularly susceptible to alterations following NMs long-term exposure. For instance, in a six-month study on workers, the handling of NMs was positively correlated with decreased activity of antioxidant enzymes, and in particular SOD and GPx (Liao et al., 2014). In another study but in a similar pattern, the redox status of workers daily exposed to metal-oxide NMs was negatively affected compared to the unexposed ones, as shown by the decreased activity of SOD and GPx and by the elevated levels of 8-hydroxydeoxyguanosine (8-oxodG), a biomarker of severe DNA oxidative damage (Liou et al., 2016). Finally, in a 4-year follow-up study, the daily exposure to various NMs was followed by increased activity of SOD and GPx in the exposed employees as compared to the unexposed ones (Wu et al., 2019).

The genotoxic effects of NMs represent a burning issue, as the somatic mutations may lead to cancer, whereas the germline mutations can be inherited by the descendants, thus provoking genetic disorders (Kohl et al., 2020). After NMs cellular uptake, two mechanisms of genotoxicity may occur; the primary, referring to the genetic damage caused by the NM itself or other intermediate biomolecules, and the secondary, resulting from ROS produced by phagocytes during the inflammatory responses in NMs presence (Samadian et al., 2020). Considering that the main mechanism of *in vivo* genotoxicity is suggested to be the secondary, the *in vivo* models are much more representative, and as a result they constitute a valuable tool to obtain a better perspective on NMs genotoxic effects (Evans et al., 2017). In addition to their *in vitro* applications, the micronucleus test, the chromosome aberration test and the comet assay are widely applied for the *in vivo* testing (Magdolenova et al., 2014). Towards this end, the peripheral blood mononuclear cells (PBMCs) and the bone marrow cells (BMCs) of rodents exposed to NMs are commonly combined with the above mentioned assays in order to assess the *in vivo* genotoxic effects (Dobrzyńska et al., 2014; Maser et al., 2015; Ghosh et al., 2016; Kazimirova et al., 2019).

Since clinical case studies regarding accidental human exposure to NMs either occupational or in everyday life are generally lacking, laboratory animals are widely used to extrapolate findings (Prabhakar et al., 2012; Ema et al., 2017; Zamboni et al., 2018). Among the different animal models, rodents, mainly mice and rats, are extensively used in biomedical research due to the positive correlation of their anatomy, physiology and genetic background with humans (Bryda, 2013). The experimental animals can be exposed to the test NMs through different routes and for various exposure times, depending on the selected exposure scenario. For inhalation studies, the experimental animals can be exposed to the test NM in an aerosol form in specially designed chambers (Yi et al., 2013; Oberdörster and Kuhlbusch, 2018), whereas in the case of ingestion studies, the NM of interest can be incorporated in the food of the experimental animals (Howard and Murashov, 2018). Finally, the topic application of the test NM on the skin of the experimental animals is the main strategy followed in the case of dermal studies (Delouise, 2012). Then, the effects of NMs are evaluated using biomarkers extensively applied for the assessment of redox status.

The use of redox biomarkers has been applied in both animals (Papadopoulou et al., 2017; Kafantaris et al., 2018; Makri et al., 2018; Fountoucidou et al., 2019) and humans (Matthaiou et al., 2014; de Wilhelmi de Toledo et al., 2020). However, the main advantage of animal models is that they provide the potentiality to evaluate redox-related parameters directly in the preferred tissue (Veskoukis et al., 2016). Although the redox biomarkers of blood reflect the tissue redox status, where heart, liver and muscle are the tissues showing the greatest correlation (Veskoukis et al., 2009; Margaritelis et al., 2015), the combined evaluation of blood and tissue redox status is directed to holistically unravel the systemic actions of NMs. Regarding NMs study, several redox parameters of animal models have been evaluated previously (Martinsda et al., 2017; Reddy et al., 2017; Docea et al., 2020; Majewski et al., 2020).

In the present approach, the effects of NMs on the redox state of blood and tissues can be evaluated via a battery of redox biomarkers previously proposed by our research group (Veskoukis et al., 2016, 2019). In particular, two categories of translational biomarkers, including biomarkers of antioxidant capacity and biomarkers of oxidative damage, are determined spectrophotometrically for the comprehensive evaluation of the redox status. The first category consists of the antioxidant molecule GSH, a panel of antioxidant enzymes, comprising SOD, CAT, GPx and GR, as well as the crude biomarker TAC. Briefly, the catalytic activity of SOD, the most powerful cell antioxidant, is responsible for the dismutation of superoxide anion to hydrogen peroxide and molecular oxygen (Ighodaro and Akinloye, 2018). Furthermore, the catalytic activity of CAT leads to the conversion of excessive hydrogen peroxide to molecular oxygen and water (Shangari and O'Brien, 2006). Likewise, GPx is implicated in the reduction of hydrogen peroxide, when it is present in low levels, using GSH as an electron donor (Margis et al., 2008). Finally, the organisms that use GSH for the maintenance of redox homeostasis are not only able to synthesize it, but they are also characterized by the ability to recycle it from its oxidized form (GSSG) via the catalytic activity of GR (Piggott and Karuso, 2007; Couto et al., 2016). On the contrary, the second category comprises biomarkers of severe oxidative damage in biomolecules, namely TBARS and protein carbonyls, which have been described previously. The preparation of blood and tissues and the proposed protocols are presented in detail within the section 4.1 and 4.2, respectively.

4.1. Tissue homogenization & blood preparation

In an EDTA tube, 500 ml of whole blood is added and centrifuged (1380 g, 10 min, 4 °C) in order to be separated into plasma and erythrocytes. Thereafter, plasma is collected and the packed erythrocytes are hemolyzed with an equal amount of dH_2O (1:1 v/v). After hemolysis, the samples are centrifuged (4000 g, 15 min, 4 °C), and the supernatant, which is the red blood cell lysate (RBCL), is collected. The RBCL is stored in separate aliquots at −80 °C, until further analysis.

Regarding tissues, they are excised, frozen immediately in liquid nitrogen (−196 °C) and kept at −80 °C, until further analysis. The homogenization process requires the weighing of the tissues and the addition of PBS containing protease inhibitors. Afterward, the samples are homogenized and centrifuged (15000 g, 5 min, 5 °C). The tissue homogenate is collected and stored in separate aliquots at −80 °C, until further analysis.

4.2. Determination of redox biomarkers by spectrophotometry

The redox biomarkers of plasma and tissue homogenates are normalized to total protein concentration, which can be measured by the Bradford assay. On the other hand, in order to normalize the redox biomarkers of RBCL, hemoglobin (Hb) concentration can be measured according to a commercially available kit.

4.2.1. Reduced glutathione (GSH)

4.2.1.1. Selected assay. Regarding GSH concentration, we propose the method of Reddy et al. (2004), as presented formerly by Veskoukis et al. (2016).

4.2.1.2. Principle of the assay. The GSH that is present in biological samples, is oxidized by the addition of 5,5-dithiobis (2-nitrobenzoic acid) (DTNB), and the resulting reaction products consist of GSSG and 2-nitro-5-thiobenzoic acid (TNB), a colored ion with maximum absorption at 412 nm.

4.2.1.3. Protocol. In detail, 500 μl of RBCL or 50 μl of tissue homogenate is mixed with 500 μl or 50 μl of 5% TCA, respectively, centrifuged (15000 g, 5 min, 5 °C) and the pure supernatant is collected. With respect to RBCL, 300 μl of the supernatant is mixed with 90 μl of 5% TCA and centrifuged once again. Afterward, 20 μl of supernatant for the samples or 20 μl of dH_2O or PBS for the controls of RBCL and tissue homogenate, respectively, is added to test tubes, followed by the addition of 660 μl of phosphate buffer (67 mM, pH = 7.95) and 330 μl of DTNB (1 mM). The samples are vortexed and incubated for 15 min in the dark at RT. After that, the absorbance is monitored at 412 nm. The millimolar extinction coefficient of DTNB (13.6 l/mmol/cm) is used for the calculation of GSH concentration, which is presented as mmol GSH/g Hb for the RBCL and as mmol GSH/mg protein for the various tissues.

4.2.2. Total antioxidant capacity (TAC)

4.2.2.1. Selected assay. For the determination of TAC levels, we propose the method of Janaszewska and Bartosz (2002).

4.2.2.2. Principle of the assay. The principle of the assay has been described above.

4.2.2.3. Protocol. In test tubes, 20 μl of plasma or 40 μl of tissue homogenate is mixed with 480 μl or 460 μl of phosphate buffer (10 mM, pH = 7.4), respectively and 500 μl of a $DPPH^{\bullet}$ solution (0.1 mM) in MeOH. It has to be noted that depending on whether the method is performed in blood or tissues, 20 μl of dH_2O or 40 μl of PBS, respectively are used as a control. Then, the samples are vortexed and incubated for 1 h in the dark at RT. Thereafter, a centrifugation (15000 g, 3 min, 25 °C) is required, and the absorbance is monitored at 520 nm. The levels of TAC are expressed as mmol DPPH/mg protein.

4.2.3. Superoxide dismutase (SOD)

4.2.3.1. Selected assay. Concerning SOD activity, we propose the method of Oberley and Spitz (1984) with some modifications.

4.2.3.2. Principle of the assay. The system of xanthine/xanthine oxidase is used for the generation of $O_2^{\bullet-}$, which are capable of reducing NBT. Nevertheless, the catalytic activity of SOD leads to the dismutation of $O_2^{\bullet-}$ to H_2O_2 and molecular oxygen, thus inhibiting NBT reduction.

4.2.3.3. Protocol. Prior to the assay, a master mix is prepared containing 13,8 ml of diethylenetriaminepentaacetic acid (DETAPAC) (1.34 mM) in potassium phosphate buffer (0.05 M, pH = 7.8), 0.5 ml of NBT (2.24 mM) in potassium phosphate buffer and 1.7 ml of xanthine (1.18 mM) in potassium phosphate buffer. Concerning the assay, in test tubes, 100 μl of RBCL (diluted 1/200) is added to 800 μl of master mix. Furthermore, a control is prepared consisting of 100 μl of DETAPAC and 800 μl of master mix. The samples are vortexed and 100 μl of xanthine oxidase (60 mU) in DETAPAC is added. Subsequently, the absorbance is monitored at 560 nm for 1.5 min. The activity of SOD is calculated on the basis of the percentage inhibition of NBT and the results are expressed as U/g Hb.

4.2.4. Catalase (CAT)

4.2.4.1. Selected assay. With respect to CAT activity, we propose the method of Aebi (1984), as mentioned previously by Veskoukis et al. (2016).

4.2.4.2. Principle of the assay. The addition of H_2O_2 to RBCL or tissue homogenate, leads to its decomposition to water and molecular oxygen via the catalytic activity of the catalase present in the biological sample. Since H_2O_2 absorbs maximal at 240 nm, the absorbance is decreased.

4.2.4.3. Protocol. Concerning the assay, 4 μl of RBCL or 40 μl of tissue homogenate are mixed with 2991 μl or 2955 μl of phosphate buffer (67 mM, pH = 7.4), respectively. Then, the samples are vortexed and placed to a laboratory incubator for 10 min at 37 °C. Subsequently, each sample is transferred in a UV quartz cuvette, 5 μl of 30% H_2O_2 is added, and the absorbance is monitored at 240 nm for 2 min. Finally, the molar extinction coefficient of H_2O_2 (40 l/mol/cm) is used for the measurement of CAT activity, which is expressed as U/g Hb for the RBCL and U/mg protein for the tissues.

4.2.5. Glutathione peroxidase (GPx)

4.2.5.1. Selected assay. For the determination of GPx activity, we propose the protocol of Flohé and Günzler (1984), as described formerly by Veskoukis et al. (2016).

4.2.5.2. Principle of the assay. GSSG derived from the catalytic activity of GPx is regenerated to GSH by the excessive activity of GR, using NADPH as a hydrogen donor. The simultaneous oxidation of NADPH is observed through an absorbance decrease at 340 nm.

4.2.5.3. Protocol. In test tubes, 100 μl of RBCL (diluted 1/100) is added to 500 μl of phosphate buffer (100 mM, pH = 7), 100 μl of glutathione reductase (GR) (0.24 U) and 100 μl of GSH (10 mM), and the mixture is incubated for 10 min at RT. Then, the content of the tube is transferred in a cuvette, followed by the addition of 100 μl of NADPH (1.5 mM) in a 0.1% $NaHCO_3$ solution, and the NADPH consumption is monitored at 340 nm for 3 min. After that, 100 μl of a tert-Butyl hydroperoxide (t-BuOOH) solution (12 mM) is added to the sample, and the consequent decrease in absorbance is monitored at 340 nm for 2.5 min. For the assessment of the non-enzymatic reaction rate, the enzyme sample is replaced by buffer. To calculate the activity of GPx, the molar extinction coefficient of NADPH (6200 l/mol/cm) is used, and the results are presented as U/g Hb.

4.2.6. Glutathione reductase (GR)

4.2.6.1. Selected assay. Regarding GR activity, we propose the protocol of Smith et al. (1988), as reported previously by Veskoukis et al. (2016).

4.2.6.2. Principle of the assay. The catalytic activity of GR is responsible for the regeneration of GSH by GSSG, and the consequent reaction of GSH with DTNB leads to the formation of TNB, which absorbs maximal at 412 nm.

4.2.6.3. Protocol. In test tubes, 700 μl of phosphate buffer (200 mM, 1 mM EDTA, pH = 7.5), 250 μl of DTNB (3 mM) in phosphate buffer and 50 μl of β-NADPH (2 mM) in phosphate buffer are added and vortexed. Subsequently, the content of the tube is transferred in a cuvette, and 50 μl of GSSG (20 mM) in phosphate buffer is added along with 25 μl of the RBCL (diluted 1/100) for the sample or 25 μl of GR (1 U/ml) for the control. By this way, the reaction is initiated, and an absorbance increase is monitored at 412 nm for 30 s. The results are presented as U/g Hb.

4.2.7. Thiobarbituric acid reactive substances (TBARS)

4.2.7.1. Selected assay. Concerning TBARS levels, we propose the method of Keles et al. (2001) with some slight modifications.

4.2.7.2. Principle of the assay. The principle of the assay has been described above.

4.2.7.3. Protocol. To begin with, 100 μl of plasma or 50 μl of tissue homogenate is added to falcon tubes and mixed with 500 μl of 35% TCA and 500 μl of Tris-HCL (200 mM, pH = 7.4). The samples are vortexed and incubated for 10 min at RT. In each experiment, 100 μl of dH_2O or 50 μl of PBS is used as a control for plasma and tissue homogenates, respectively. Thereafter, 1 ml of a solution consisting of Na_2SO_4 (2 M) and TBA (55 mM) is added, and the samples are placed in a water bath for 45 min at 95 °C. After incubation, the samples are transferred on ice for 5 min, in order to be cooled, 1 ml of 70% TCA is added, and the samples are vortexed and centrifuged (11200 g, 3 min, 25 °C). Finally, the absorbance is monitored at 530 nm. The concentration of TBARS is presented as μmol TBARS/mg protein.

4.2.8. Protein carbonyls

4.2.8.1. Selected assay. To determine the concentration of protein carbonyls, we propose the method of Patsoukis et al. (2004), as described formerly by Veskoukis et al. (2016).

4.2.8.2. Principle of the assay. The principle of the assay has been described above.

4.2.8.3. Protocol. In test tubes, 50 μl of plasma or tissue homogenate is mixed with 50 μl of 20% TCA, and the mixture is transferred in ice bath for 15 min, followed by a centrifugation (15000 g, 5 min, 4 °C). Then, the supernatant is disposed and 500 μl of a DNPH solution (10 mM) (in 2.5N HCl) or 500 μl of HCl (2.5N) is added to the samples and the controls, respectively. Each sample has its own control. The samples are incubated for 1 h in the dark at RT, vortexed intermittently every 15 min and centrifuged (15000 g, 5 min, 4 °C). Subsequently, the supernatant is discarded, 1 ml of 10% TCA is added, and the samples are vortexed and centrifuged (15000 g, 5 min, 4 °C). After centrifugation, the supernatant is discarded, 1 ml of a mixture containing ethanol-ethyl acetate (1:1 v/v) is added, and the samples are vortexed and centrifuged (15000 g, 5 min, 4 °C). The aforementioned step is repeated twice. Subsequently, the supernatant is discarded, the samples are treated with 1 ml of urea (5 M, pH = 2.3), vortexed and transferred to an incubator for 15 min at 37 °C. Following incubation, the samples are centrifuged (15000 g, 3 min, 4 °C), and the absorbance is monitored at 375 nm. Protein carbonyls concentration is presented as nmol protein carbonyls/mg protein.

5. Conclusion

Nanotechnology represents one of the most promising and novel technological frontiers, and NMs are at the leading edge of this rapidly developing field, since their unique physicochemical characteristics provide multiple advantages, as compared to the corresponding bulk materials. In this regard, the use of NMs is prevalent in a multitude of industrial applications and consumer products. Obviously, the increasing production and use of NMs, which is expected to intensify even more in the near future, leads to greater exposure levels of both humans and environment. Besides the workers, exposed to NMs during the whole production process, the general population is also exposed via the release of NMs throughout the life cycle of nanotechnology products. Additionally, the fate of NMs in the natural environment is critical, since except the environmental effects, humans are re-exposed through the direct contact with it. Due to the relatively recent emergence, the effects of NMs on human health and safety are not yet fully understood. Nevertheless, scientific evidence indicates that the effects of NMs on biological entities are often associated with their redox-related properties, and consequently their evaluation is of great importance in order to reveal their impact on human health. To date, it is well known that the pathophysiology of various diseases is redox-related, and the generation of excess free radicals, followed by the induction of oxidative stress is a direct outcome of them. Despite the fact that oxidative stress is present in these pathological conditions, it is not yet known if it represents just a clinical outcome or even a provoking factor linked to the disease onset. In this context, it requires further investigation whether the chronic exposure to low levels of NMs is capable of inducing toxicity via this mechanism, thus promoting the onset of diseases associated with the imbalance of redox equilibrium. Based on the above, we have proposed a comprehensive approach for the evaluation of the redox-related effects of NMs at three biological levels, using translational redox biomarkers. Moreover, we have recommended a series of protocols, the most reliable and valid, according to our opinion, for the determination of the proposed redox biomarkers. The approach is expected to be a useful tool, which will contribute to obtain a better understanding regarding NMs biological effects and to shed light on the potential risk arising from the increasing human exposure to them.

Author contributions

Periklis Vardakas: Methodology, Visualization, Writing - original draft. Zoi Skaperda: Methodology, Visualization, Writing - review & editing. Fotios Tekos: Methodology, Visualization, Writing - review & editing. Aikaterini-Flora Trompeta: Visualization, Writing - review & editing. Aristidis Tsatsakis: Conceptualization, Writing - review & editing. Constantinos A. Charitidis: Conceptualization, Visualization, Writing - review & editing. Demetrios Kouretas: Conceptualization, Project administration, Supervision.

Declaration of competing interest

The authors declare that they have no known competing financial interests or personal relationships that could have appeared to influence the work reported in this paper.

Acknowledgements

This study has been funded by the Horizon 2020 Project "DECOAT" (Recycling of coated and painted textile and plastic materials) under G. A. 814505.

References

Aebi, H., 1984. [13] catalase in vitro. Methods Enzymol. 105 (C), 121–126. https://doi.org/10.1016/S0076-6879(84)05016-3.
Al-Lamki, R.S., Bradley, J.R., Pober, J.S., 2017. Human organ culture: updating the approach to bridge the gap from in vitro to in vivo in inflammation, cancer, and stem cell biology. Frontiers in Medicine. Frontiers Media S.A. 1. https://doi.org/10.3389/fmed.2017.00148.
Allegri, M., et al., 2016. Toxicity determinants of multi-walled carbon nanotubes: the relationship between functionalization and agglomeration. Toxicology Reports 3, 230–243. https://doi.org/10.1016/j.toxrep.2016.01.011.
Apostolou, A., et al., 2013. Assessment of polyphenolic content, antioxidant activity, protection against ROS-induced DNA damage and anticancer activity of Vitis vinifera stem extracts. Food Chem. Toxicol. 61, 60–68. https://doi.org/10.1016/j.fct.2013.01.029.
Aquilano, K., Baldelli, S., Ciriolo, M.R., 2014. Glutathione: new roles in redox signalling for an old antioxidant. In: Frontiers in Pharmacology. Frontiers Research Foundation. https://doi.org/10.3389/fphar.2014.00196.
Ayala, A., Muñoz, M.F., Argüelles, S., 2014. Lipid peroxidation: Production, metabolism, and signaling mechanisms of malondialdehyde and 4-hydroxy-2-nonenal. Oxid. Med. Cell. Longev. Landes Biosci. https://doi.org/10.1155/2014/360438.
Bakand, S., Hayes, A., 2016. Toxicological considerations, toxicity assessment, and risk management of inhaled nanoparticles. *International Journal of Molecular Sciences*. MDPI AG. https://doi.org/10.3390/ijms17060929.
Bakshi, M.S., 2020. 'Impact of Nanomaterials on Ecosystems: Mechanistic Aspects in Vivo', *Environmental Research*. Academic Press Inc., p. 109099. https://doi.org/10.1016/j.envres.2019.109099
Balasubramanyam, A., et al., 2010. In vitro mutagenicity assessment of aluminium oxide nanomaterials using the Salmonella/microsome assay. Toxicol. Vitro 24 (6), 1871–1876. https://doi.org/10.1016/j.tiv.2010.07.004.
Balmuri, S.R., et al., 2017. Effect of surfactant in mitigating cadmium oxide nanoparticle toxicity: implications for mitigating cadmium toxicity in environment. Environ. Res. 152, 141–149. https://doi.org/10.1016/j.envres.2016.10.005.
Berdiaki, A., et al., 2020. 'Assessment of amphiphilic poly- N-vinylpyrrolidone nanoparticles' biocompatibility with endothelial cells in vitro and delivery of an anti-inflammatory drug'. Mol. Pharm. 17 (11), 4212–4225. https://doi.org/10.1021/acs.molpharmaceut.0c00667.
Bondavalli, P., et al., 2019. Deposition of graphene and related nanomaterials by dynamic spray-gun method: a new route to implement nanomaterials in real applications. J. Phys.: Materials 2 (3), 032002. https://doi.org/10.1088/2515-7639/ab1795.
Bostan, H.B., et al., 2016. 'Cardiotoxicity of Nano-Particles', *Life Sciences*. Elsevier Inc., pp. 91–99. https://doi.org/10.1016/j.lfs.2016.09.017
Bouwmeester, H., van der Zande, M., Jepson, M.A., 2018. Effects of food-borne nanomaterials on gastrointestinal tissues and microbiota. Wiley Interdisciplinary Reviews: Nanomedicine and Nanobiotechnology 10 (1), e1481. https://doi.org/10.1002/wnan.1481.
Boverhof, D.R., et al., 2015. Comparative assessment of nanomaterial definitions and safety evaluation considerations. Regul. Toxicol. Pharmacol. 73 (1), 137–150. https://doi.org/10.1016/j.yrtph.2015.06.001.
Bradford, M., 1976. A rapid and sensitive method for the quantitation of microgram quantities of protein utilizing the principle of protein-dye binding. Anal. Biochem. 72 (1–2), 248–254. https://doi.org/10.1006/abio.1976.9999.
Brand-Williams, W., Cuvelier, M.E., Berset, C., 1995. Use of a free radical method to evaluate antioxidant activity. LWT - Food Sci. Technol. (Lebensmittel-Wissenschaft -Technol.) 28 (1), 25–30. https://doi.org/10.1016/S0023-6438(95)80008-5.
Breznan, D., et al., 2015. Non-specific interaction of carbon nanotubes with the resazurin assay reagent: impact on in vitro assessment of nanoparticle cytotoxicity. Toxicol. Vitro 29 (1), 142–147. https://doi.org/10.1016/j.tiv.2014.09.009.
Bryda, E.C., 2013. The Mighty Mouse: the impact of rodents on advances in biomedical research. Mo. Med. 110 (3), 207–211.

Cano, A., Acosta, M., Arnao, M.B., 2000. A method to measure antioxidant activity in organic media: application to lipophilic vitamins. Redox Rep. 5 (6), 365–370. https://doi.org/10.1179/135100000101535933.
Chia, S.L., et al., 2015. Biomimicry 3D gastrointestinal spheroid platform for the assessment of toxicity and inflammatory effects of zinc oxide nanoparticles. Small 11 (6), 702–712. https://doi.org/10.1002/smll.201401915.
Chung, S. -K., Osawa, T., Kawakishi, S., 1997. Hydroxyl radical-scavenging effects of spices and scavengers from brown mustard (brassica nigra). Biosci. Biotechnol. Biochem. 61 (1), 118–123. https://doi.org/10.1271/bbb.61.118.
Contado, C., 2015. Nanomaterials in consumer products: a challenging analytical problem. In: Frontiers in Chemistry. Frontiers Media S. A, p. 48. https://doi.org/10.3389/fchem.2015.00048.
Coricovac, D.E., et al., 2017. Biocompatible colloidal suspensions based on magnetic iron oxide nanoparticles: synthesis, characterization and toxicological profile. Front. Pharmacol. 8 (MAR) https://doi.org/10.3389/fphar.2017.00154.
Couto, N., Wood, J., Barber, J., 2016. The role of glutathione reductase and related enzymes on cellular redox homoeostasis network. Free Radical Biology and Medicine. Elsevier Inc., pp. 27–42. https://doi.org/10.1016/j.freeradbiomed.2016.02.028
Csányi, G., Miller, F.J., 2014. Oxidative stress in cardiovascular disease. Int. J. Mol. Sci. 15 (4), 6002–6008. https://doi.org/10.3390/ijms15046002.
Da Rocha, E.L., Porto, L.M., Rambo, C.R., 2014. Nanotechnology meets 3D in vitro models: Tissue engineered tumors and cancer therapies. Elsevier, pp. 270–279. https://doi.org/10.1016/j.msec.2013.09.019.
Dayem, A.A., et al., 2017. The role of reactive oxygen species (ROS) in the biological activities of metallic nanoparticles. *International Journal of Molecular Sciences*. MDPI AG 120. https://doi.org/10.3390/ijms18010120.
Dellinger, A., et al., 2013. 'Application of Fullerenes in Nanomedicine: an Update', *Nanomedicine*. Future Medicine Ltd., pp. 1191–1208. https://doi.org/10.2217/nnm.13.99
Delouise, L.A., 2012. Applications of nanotechnology in dermatology. J. Invest. Dermatol. 964–975. https://doi.org/10.1038/jid.2011.425. Nature Publishing Group.
Dhall, A., Self, W., 2018. Cerium oxide nanoparticles: a brief review of their synthesis methods and biomedical applications. Antioxidants 7 (8), 97. https://doi.org/10.3390/antiox7080097.
Dobrzyńska, M.M., et al., 2014. Genotoxicity of silver and titanium dioxide nanoparticles in bone marrow cells of rats in vivo. Toxicology 315 (1), 86–91. https://doi.org/10.1016/j.tox.2013.11.012.
Docea, A.O., et al., 2018. 'Six months exposure to a real life mixture of 13 chemicals' below individual NOAELs induced non monotonic sex-dependent biochemical and redox status changes in rats'. Food Chem. Toxicol. 115, 470–481. https://doi.org/10.1016/j.fct.2018.03.052.
Docea, A.O., et al., 2020. The effect of silver nanoparticles on antioxidant/pro-oxidant balance in a murine model. Int. J. Mol. Sci. 21 (4), 1233. https://doi.org/10.3390/ijms21041233.
Drasler, B., et al., 2017. In Vitro Approaches to Assess the Hazard of Nanomaterials. *NanoImpact*. Elsevier B.V., pp. 99–116. https://doi.org/10.1016/j.impact.2017.08.002
Du, X., et al., 2019. Genotoxicity evaluation of titanium dioxide nanoparticles using the mouse lymphoma assay and the Ames test. Mutat. Res. Genet. Toxicol. Environ. Mutagen 838, 22–27. https://doi.org/10.1016/j.mrgentox.2018.11.015.
Edmondson, R., et al., 2014. Three-dimensional cell culture systems and their applications in drug discovery and cell-based biosensors. In: Assay and Drug Development Technologies. Mary Ann Liebert Inc., pp. 207–218. https://doi.org/10.1089/adt.2014.573
Elespuru, R., et al., 2018. Genotoxicity assessment of nanomaterials: recommendations on best practices, assays, and methods. Toxicol. Sci. 164 (2), 391–416. https://doi.org/10.1093/toxsci/kfy100.
Ema, M., et al., 2017. 'A Review of Reproductive and Developmental Toxicity of Silver Nanoparticles in Laboratory Animals', *Reproductive Toxicology*. Elsevier Inc., pp. 149–164. https://doi.org/10.1016/j.reprotox.2017.01.005
Engin, A.B., et al., 2017. 'Mechanistic Understanding of Nanoparticles' Interactions with Extracellular Matrix: the Cell and Immune System', *Particle and Fibre Toxicology*. BioMed Central Ltd., pp. 1–16. https://doi.org/10.1186/s12989-017-0199-z
Evans, S.J., et al., 2017. Critical Review of the Current and Future Challenges Associated with Advanced in Vitro Systems towards the Study of Nanoparticle (Secondary) Genotoxicity. Oxford University Press, Mutagenesis, pp. 233–241. https://doi.org/10.1093/mutage/gew054.
Fang, Y., Eglen, R.M., 2017. 'Three-Dimensional Cell Cultures in Drug Discovery and Development', *SLAS Discovery*. Oxford University Press, pp. 456–472. https://doi.org/10.1177/1087057117696795.
Fenoglio, I., et al., 2006. Reactivity of carbon nanotubes: free radical generation or scavenging activity? Free Radic. Biol. Med. 40 (7), 1227–1233. https://doi.org/10.1016/j.freeradbiomed.2005.11.010.
Ferreira, C.A., et al., 2018. Scavenging of reactive oxygen and nitrogen species with nanomaterials. In: Nano Research. Tsinghua University Press, pp. 4955–4984. https://doi.org/10.1007/s12274-018-2092-y.
Figueiredo Borgognoni, C., et al., 2018. 'Human macrophage responses to metal-oxide nanoparticles: a review', *Artificial Cells*. Nanomedicine, and Biotechnology 46 (Suppl. 2), 694–703. https://doi.org/10.1080/21691401.2018.1468767.
Flohé, L., Günzler, W.A., 1984. [12] assays of glutathione peroxidase. Methods Enzymol. 105 (C), 114–120. https://doi.org/10.1016/S0076-6879(84)05015-1.
Forest, V., et al., 2015. Adsorption of lactate dehydrogenase enzyme on carbon nanotubes: how to get accurate results for the cytotoxicity of these nanomaterials. Langmuir 31 (12), 3635–3643. https://doi.org/10.1021/acs.langmuir.5b00631.
Fountoucidou, P., et al., 2019. A mixture of routinely encountered xenobiotics induces both redox adaptations and perturbations in blood and tissues of rats after a long-term low-dose exposure regimen: the time and dose issue. Toxicol. Lett. 317, 24–44. https://doi.org/10.1016/j.toxlet.2019.09.015.
Fu, P.P., et al., 2014. Mechanisms of nanotoxicity: generation of reactive oxygen species. Journal of Food and Drug Analysis. Elsevier Taiwan LLC 64–75. https://doi.org/10.1016/j.jfda.2014.01.005.
Gajanan, K., Tijare, S.N., 2018. Applications of nanomaterials. In: Materials Today: Proceedings. Elsevier Ltd, pp. 1093–1096. https://doi.org/10.1016/j.matpr.2017.11.187.
Gao, X., Lowry, G.V., 2018. Progress towards Standardized and Validated Characterizations for Measuring Physicochemical Properties of Manufactured Nanomaterials Relevant to Nano Health and Safety Risks. *NanoImpact*. Elsevier B.V., pp. 14–30. https://doi.org/10.1016/j.impact.2017.09.002
Gatoo, M.A., et al., 2014. 'Physicochemical Properties of Nanomaterials: Implication in Associated Toxic Manifestations', *BioMed Research International*. Hindawi Publishing Corporation. https://doi.org/10.1155/2014/498420.
Genc, N., 2020. Biosynthesis of Silver Nanoparticles Using Origanum Onites Extract and Investigation of Their Antioxidant Activity. Particulate Science and Technology, pp. 1–7. https://doi.org/10.1080/02726351.2020.1786868.
Ghosh, M., et al., 2016. Cyto-genotoxicity and oxidative stress induced by zinc oxide nanoparticle in human lymphocyte cells in vitro and Swiss albino male mice in vivo. Food Chem. Toxicol. 97, 286–296. https://doi.org/10.1016/j.fct.2016.09.025.
Gonos, E.S., et al., 2018. 'Origin and Pathophysiology of Protein Carbonylation, Nitration and Chlorination in Age-Related Brain Diseases and Aging', *Aging*. Impact Journals LLC, pp. 868–901. https://doi.org/10.18632/aging.101450.
Goutzourelas, N., et al., 2015. Polyphenolic composition of grape stem extracts affects antioxidant activity in endothelial and muscle cells. Mol. Med. Rep. 12 (4), 5846–5856. https://doi.org/10.3892/mmr.2015.4216.
Grundler, F., et al., 2020. Interplay between oxidative damage, the redox status, and metabolic biomarkers during long-term fasting. Food Chem. Toxicol. 145, 111701. https://doi.org/10.1016/j.fct.2020.111701.
Gülçin, I., et al., 2004. Antioxidant, antimicrobial, antiulcer and analgesic activities of nettle (Urtica dioica L.). J. Ethnopharmacol. 90 (2–3), 205–215. https://doi.org/10.1016/j.jep.2003.09.028.
Haase, A., Luch, A., 2016. Genotoxicity of nanomaterials in vitro: treasure or trash?. In: Archives of Toxicology. Springer Verlag, pp. 2827–2830. https://doi.org/10.1007/s00204-016-1825-5.
Hecker, L., 2018. Mechanisms and consequences of oxidative stress in lung disease: therapeutic implications for an aging populace. Am. J. Physiol. Lung Cell Mol. Physiol.. American Physiological Society L642–L653. https://doi.org/10.1152/ajplung.00275.2017.
Hoskins, C., et al., 2012. Dilemmas in the reliable estimation of the in-vitro cell viability in magnetic nanoparticle engineering: which tests and what protocols? Nanoscale Research Letters 7 (1), 77. https://doi.org/10.1186/1556-276X-7-77.
Howard, J., Murashov, V., 2018. Use of nanomaterials in animals. Applied Biosafety 23 (3), 162–167. https://doi.org/10.1177/1535676018771984.
Hussain, S., et al., 2014. Intracellular signal modulation by nanomaterials. Adv. Exp. Med. Biol. 811, 113–134. https://doi.org/10.1007/978-94-017-8739-0_7.
Ighodaro, O.M., Akinloye, O.A., 2018. First line defence antioxidants-superoxide dismutase (SOD), catalase (CAT) and glutathione peroxidase (GPX): their fundamental role in the entire antioxidant defence grid. Alexandria Journal of Medicine 54 (4), 287–293. https://doi.org/10.1016/j.ajme.2017.09.001.
Janaszewska, A., Bartosz, G., 2002. Assay of total antioxidant capacity: comparison of four methods as applied to human blood plasma. Scand. J. Clin. Lab. Investig. 62 (3), 231–236. https://doi.org/10.1080/003655102317475498.
Jeevanandam, J., et al., 2018. Review on nanoparticles and nanostructured materials: history, sources, toxicity and regulations. In: Beilstein Journal of Nanotechnology. Beilstein-Institut Zur Forderung der Chemischen Wissenschaften, pp. 1050–1074. https://doi.org/10.3762/bjnano.9.98.
Kabir, E., et al., 2018. Environmental impacts of nanomaterials. J. Environ. Manag. 261–271. https://doi.org/10.1016/j.jenvman.2018.07.087. Academic Press.
Kafantaris, I., et al., 2018. Grape pomace improves performance, antioxidant status, fecal microbiota and meat quality of piglets. Animal 12 (2), 246–255. https://doi.org/10.1017/S1751731117001604.
Kausar, A., 2019. Nanomaterials in environmental protection. American Journal of Environmental Science & Technology (3), 1–10.
Kazimirova, A., et al., 2019. Titanium dioxide nanoparticles tested for genotoxicity with the comet and micronucleus assays in vitro, ex vivo and in vivo. Mutat. Res. Genet. Toxicol. Environ. Mutagen 843, 57–65. https://doi.org/10.1016/j.mrgentox.2019.05.001.
Keles, M.S., et al., 2001. Effect of corticosteroid therapy on serum and CSF malondialdehyde and antioxidant proteins in multiple sclerosis. Can. J. Neurol. Sci. 28 (2), 141–143. https://doi.org/10.1017/S0317167100052823.
Kerasioti, E., et al., 2014. Antioxidant effects of whey protein on muscle C2C12 cells. Food Chem. 155, 271–278. https://doi.org/10.1016/j.foodchem.2014.01.066.
Kerasioti, E., et al., 2020. The flavoring and not the nicotine content is a decisive factor for the effects of refill liquids of electronic cigarette on the redox status of endothelial cells. Toxicology Reports 7, 1095–1102. https://doi.org/10.1016/j.toxrep.2020.08.029.
Kerasioti, E., Stagos, D., Tzimi, A., Kouretas, D., 2016. Increase in antioxidant activity by sheep/goat whey protein through nuclear factor-like 2 (Nrf2) is cell type dependent. Food Chem. Toxicol. 97, 47–56. https://doi.org/10.1016/j.fct.2016.08.022.
Kirichenko, K., et al., 2019. Dependence of welding fume particle toxicity on electrode type and current intensity assessed by microalgae growth inhibition test. Environ. Res. 179 (Pt B), 108818. https://doi.org/10.1016/j.envres.2019.108818.

Klaper, R.D., 2020. The known and unknown about the environmental safety of nanomaterials in commerce. Small 16 (36), 2000690. https://doi.org/10.1002/smll.202000690.

Kobayashi, A., et al., 2006. Oxidative and electrophilic stresses activate Nrf2 through inhibition of ubiquitination activity of Keap1. Mol. Cell Biol. 26 (1), 221–229. https://doi.org/10.1128/mcb.26.1.221-229.2006.

Kohl, Y., et al., 2020. 'Genotoxicity of nanomaterials: advanced in vitro models and high throughput methods for human hazard assessment—a review'. Nanomaterials 1–25. https://doi.org/10.3390/nano10101911. MDPI AG.

Koledova, Z., 2017. 3D cell culture: an introduction. In: Methods in Molecular Biology. Humana Press Inc., pp. 1–11. https://doi.org/10.1007/978-1-4939-7021-6_1

Kouka, P., et al., 2017. Assessment of the antioxidant activity of an olive oil total polyphenolic fraction and hydroxytyrosol from a Greek Olea europea variety in endothelial cells and myoblasts. Int. J. Mol. Med. 40 (3), 703–712. https://doi.org/10.3892/ijmm.2017.3078.

Kouka, P., et al., 2019. Olive tree blossom polyphenolic extracts exert antioxidant and antimutagenic activities in vitro and in various cell lines. Oncol. Rep. 42 (6), 2814–2825. https://doi.org/10.3892/or.2019.7386.

Kuhlbusch, T.A.J., Wijnhoven, S.W.P., Haase, A., 2018. Nanomaterial Exposures for Worker, Consumer and the General Public. *NanoImpact*. Elsevier B.V., pp. 11–25. https://doi.org/10.1016/j.impact.2017.11.003

Kunwar, A., Priyadarsini, K.I., 2011. Free radicals, oxidative stress and importance of antioxidants in human health -. J. Med. Allied Sci. 1 (2), 53–60.

Kuskov, A.N., et al., 2017. Amphiphilic poly-N-vinylpyrrolidone nanoparticles as carriers for non-steroidal, anti-inflammatory drugs: in vitro cytotoxicity and in vivo acute toxicity study. Nanomed. Nanotechnol. Biol. Med. 13 (3), 1021–1030. https://doi.org/10.1016/j.nano.2016.11.006.

Kyriakidou, K., et al., 2020. In vitro cytotoxicity assessment of pristine and carboxyl-functionalized MWCNTs. Food Chem. Toxicol. 141 https://doi.org/10.1016/j.fct.2020.111374.

Lai, T.H., et al., 2015. Gold nanoparticles induce heme oxygenase-I expression through Nrf2 activation and BachI export in human vascular endothelial cells. Int. J. Nanomed. 10, 5925–5939. https://doi.org/10.2147/IJN.S88514.

Landsiedel, R., et al., 2014. Pulmonary toxicity of nanomaterials: a critical comparison of published in vitro assays and in vivo inhalation or instillation studies. Nanomedicine 2557–2585. https://doi.org/10.2217/nnm.14.149. Future Medicine Ltd.

Larese Filon, F., et al., 2015. 'Nanoparticles skin absorption: new aspects for a safety profile evaluation'. Regul. Toxicol. Pharmacol. 310–322. https://doi.org/10.1016/j.yrtph.2015.05.005. Academic Press Inc.

Lee, J., et al., 2009. In vitro toxicity testing of nanoparticles in 3D cell culture. Small 5 (10). https://doi.org/10.1002/smll.200801788. NA-NA.

Li, Y., et al., 2012. Genotoxicity of silver nanoparticles evaluated using the Ames test and in vitro micronucleus assay. Mutat. Res. Genet. Toxicol. Environ. Mutagen 745 (1–2), 4–10. https://doi.org/10.1016/j.mrgentox.2011.11.010.

Liao, H.Y., et al., 2014. Six-month follow-up study of health markers of nanomaterials among workers handling engineered nanomaterials. Nanotoxicology 8 (Suppl. 1), 100–110. https://doi.org/10.3109/17435390.2013.858793.

Liou, S.H., et al., 2015. Assessing the first wave of epidemiological studies of nanomaterial workers. J. Nanoparticle Res. 413. https://doi.org/10.1007/s11051-015-3219-7. Kluwer Academic Publishers.

Liou, S.H., et al., 2016. Increased levels of oxidative stress biomarkers in metal oxides nanomaterial-handling workers. Biomarkers 21 (7), 600–606. https://doi.org/10.3109/1354750X.2016.1160432.

Liu, W., et al., 2017. Nrf2 protects against oxidative stress induced by SiO2 nanoparticles. Nanomedicine 12 (19), 2303–2318. https://doi.org/10.2217/nnm-2017-0046.

Liu, Y., Shi, J., 2019. Antioxidative nanomaterials and biomedical applications. Nano Today 146–177. https://doi.org/10.1016/j.nantod.2019.05.008. Elsevier B.V.

Luss, A.L., et al., 2018. Nanosized carriers based on amphiphilic poly-N-vinyl-2-pyrrolidone for intranuclear drug delivery. Nanomedicine 13 (7), 703–715. https://doi.org/10.2217/nnm-2017-0311.

Ma, Q., 2013. 'Role of Nrf2 in oxidative stress and toxicity', *annual Review of Pharmacology and toxicology*. Annu. Rev. Pharmacol. Toxicol. 401–426. https://doi.org/10.1146/annurev-pharmtox-011112-140320.

Magdolenova, Z., et al., 2014. Mechanisms of Genotoxicity. A Review of in Vitro and in Vivo Studies with Engineered Nanoparticles, pp. 233–278. https://doi.org/10.3109/17435390.2013.773464. Nanotoxicology.

Maiväli, Ü., 2015. Do we need a science of science?. In: Science Methodology and what Can Go Wrong. Elsevier, pp. 3–53. https://doi.org/10.1016/b978-0-12-418689-7.00001-6.

Majewski, M., et al., 2020. In: Bader, M. (Ed.), 'Dietary Supplementation with Copper Nanoparticles Influences the Markers of Oxidative Stress and Modulates Vasodilation of Thoracic Arteries in Young Wistar Rats', *PLOS ONE*, vol. 15, e0229282. https://doi.org/10.1371/journal.pone.0229282, 2.

Makri, S., et al., 2018. Novel feed including olive oil mill wastewater bioactive compounds enhanced the redox status of lambs. In Vivo 32 (2), 291–302. https://doi.org/10.21873/invivo.11237.

Margaritelis, N.V., et al., 2015. 'Blood reflects tissue oxidative stress: a systematic review'. Biomarkers 97–108. https://doi.org/10.3109/1354750X.2014.1002807. Informa Healthcare.

Margis, R., et al., 2008. Glutathione peroxidase family - an evolutionary overview. FEBS J. 275 (15), 3959–3970. https://doi.org/10.1111/j.1742-4658.2008.06542.x.

Maron, D.M., Ames, B.N., 1983. 'Revised methods for the Salmonella mutagenicity test'. Mutat. Res. Environ. Mutagen Relat. Subj. 173–215. https://doi.org/10.1016/0165-1161(83)90010-9. Mutat Res.

Martins A, da C., et al., 2017. Evaluation of distribution, redox parameters, and genotoxicity in Wistar rats co-exposed to silver and titanium dioxide nanoparticles. J. Toxicol. Environ. Health 80 (19–21), 1156–1165. https://doi.org/10.1080/15287394.2017.1357376.

Maser, E., et al., 2015. In vitro and in vivo genotoxicity investigations of differently sized amorphous SiO2 nanomaterials. Mutat. Res. Genet. Toxicol. Environ. Mutagen 794, 57–74. https://doi.org/10.1016/j.mrgentox.2015.10.005.

Matthaiou, C.M., et al., 2014. Pomegranate juice consumption increases GSH levels and reduces lipid and protein oxidation in human blood. Food Chem. Toxicol. 73, 1–6. https://doi.org/10.1016/j.fct.2014.07.027.

Mendoza, R.P., Brown, J.M., 2019. Engineered nanomaterials and oxidative stress: current understanding and future challenges. Current Opinion in Toxicology 74–80. https://doi.org/10.1016/j.cotox.2018.09.001. Elsevier B.V.

Meng, H., et al., 2018. 'Walking the line: the fate of nanomaterials at biological barriers'. Biomaterials 41–53. https://doi.org/10.1016/j.biomaterials.2018.04.056. Elsevier Ltd.

Mikropoulou, E.V., et al., 2018. Phytochemical composition of the decoctions of Greek edible greens (chórta) and evaluation of antioxidant and cytotoxic properties. Molecules 23 (7). https://doi.org/10.3390/molecules23071541.

Mishra, Y.K., et al., 2017. 'Progress in electronics and photonics with nanomaterials'. Vacuum 304–307. https://doi.org/10.1016/j.vacuum.2017.09.035. Elsevier Ltd.

Mrakovcic, M., et al., 2013. Assessment of long-term effects of nanoparticles in a microcarrier cell culture system. PloS One 8 (2), 56791. https://doi.org/10.1371/journal.pone.0056791.

Mylonas, C., Kouretas, D., 1999. Lipid peroxidation and tissue damage. In Vivo 13 (3), 295–309.

Nafisi, S., Maibach, H.I., 2018. Skin penetration of nanoparticles. In: Emerging Nanotechnologies in Immunology: the Design, Applications and Toxicology of Nanopharmaceuticals and Nanovaccines. Elsevier, pp. 47–88. https://doi.org/10.1016/B978-0-323-40016-9.00003-8.

Navya, P.N., Daima, H.K., 2016. Rational engineering of physicochemical properties of nanomaterials for biomedical applications with nanotoxicological perspectives. Nano Convergence 3 (1), 1. https://doi.org/10.1186/s40580-016-0064-z.

Neagu, M., et al., 2017. 'Protein bio-corona: critical issue in immune nanotoxicology'. Arch. Toxicol. 1031–1048. https://doi.org/10.1007/s00204-016-1797-5. Springer Verlag.

Ng, C.T., et al., 2010. Current studies into the genotoxic effects of nanomaterials. J. Nucleic Acids. https://doi.org/10.4061/2010/947859.

Nogueira, D., et al., 2014. Mechanisms underlying cytotoxicity induced by engineered nanomaterials: a review of in vitro studies. Nanomaterials 4 (2), 454–484. https://doi.org/10.3390/nano4020454.

Oberbek, P., et al., 2019. 'Inhalation exposure to various nanoparticles in work environment—contextual information and results of measurements'. J. Nanoparticle Res. 21 (11), 222. https://doi.org/10.1007/s11051-019-4651-x.

Oberdörster, G., Kuhlbusch, T.A.J., 2018. In Vivo Effects: Methodologies and Biokinetics of Inhaled Nanomaterials. *NanoImpact*. Elsevier B.V., pp. 38–60. https://doi.org/10.1016/j.impact.2017.10.007

Oberley, L.W., Spitz, D.R., 1984. [61] assay of superoxide dismutase activity in tumor tissue. Methods Enzymol. 105 (C), 457–464. https://doi.org/10.1016/S0076-6879(84)05064-3.

Panieri, E., et al., 2020. 'Potential applications of NRF2 modulators in cancer therapy', *Antioxidants*. MDPI AG. https://doi.org/10.3390/antiox9030193.

Papadopoulou, A., et al., 2017. Enhancement of antioxidant mechanisms and reduction of oxidative stress in chickens after the administration of drinking water enriched with polyphenolic powder from olive mill waste waters. Oxidative Medicine and Cellular Longevity. https://doi.org/10.1155/2017/8273160, 2017.

Park, M.V.D.Z., et al., 2009. The status of in vitro toxicity studies in the risk assessment of nanomaterials. *Nanomedicine*. Nanomedicine (Lond) 669–685. https://doi.org/10.2217/nnm.09.40.

Patsoukis, N., et al., 2004. Thiol redox state (TRS) and oxidative stress in the mouse hippocampus after pentylenetetrazol-induced epileptic seizure. Neurosci. Lett. 357 (2), 83–86. https://doi.org/10.1016/j.neulet.2003.10.080.

Piccinini, F., et al., 2017. Cell counting and viability assessment of 2D and 3D cell cultures: expected reliability of the trypan blue assay. Biol. Proced. Online 19 (1), 8. https://doi.org/10.1186/s12575-017-0056-3.

Pietroiusti, A., et al., 2018. Nanomaterial exposure, toxicity, and impact on human health. Wiley Interdisciplinary Reviews: Nanomedicine and Nanobiotechnology 10 (5), e1513. https://doi.org/10.1002/wnan.1513.

Pietroiusti, A., Magrini, A., Campagnolo, L., 2014. Mechanisms of nanomaterial toxicity. Health and Environmental Safety of Nanomaterials: Polymer Nanocomposites and Other Materials Containing Nanoparticles. Elsevier Ltd., pp. 28–43. https://doi.org/10.1533/9780857096678.1.28

Piggott, A.M., Karuso, P., 2007. Fluorometric assay for the determination of glutathione reductase activity. Anal. Chem. 79 (22), 8769–8773. https://doi.org/10.1021/ac071518p.

Pikula, K., et al., 2020. Aquatic toxicity and mode of action of CdS and ZnS nanoparticles in four microalgae species. Environ. Res. 186, 109513. https://doi.org/10.1016/j.envres.2020.109513.

Pikula, K.S., et al., 2018. Effects of carbon and silicon nanotubes and carbon nanofibers on marine microalgae Heterosigma akashiwo. Environ. Res. 166, 473–480. https://doi.org/10.1016/j.envres.2018.06.005.

Pinzaru, I., et al., 2018. 'Stable PEG-coated silver nanoparticles – a comprehensive toxicological profile'. Food Chem. Toxicol. 111, 546–556. https://doi.org/10.1016/j.fct.2017.11.051.

Piperigkou, Z., et al., 2016. 'Emerging aspects of nanotoxicology in health and disease: from agriculture and food sector to cancer therapeutics'. Food Chem. Toxicol. 42–57. https://doi.org/10.1016/j.fct.2016.03.003. Elsevier Ltd.
Pisoschi, A.M., Pop, A., 2015. 'The role of antioxidants in the chemistry of oxidative stress: a review'. Eur. J. Med. Chem. 55–74. https://doi.org/10.1016/j.ejmech.2015.04.040. Elsevier Masson SAS.
Prabhakar, P.V., et al., 2012. Oxidative stress induced by aluminum oxide nanomaterials after acute oral treatment in Wistar rats. J. Appl. Toxicol. 32 (6), 436–445. https://doi.org/10.1002/jat.1775.
Priftis, A., et al., 2015. Comparison of antioxidant activity between green and roasted coffee beans using molecular methods. Mol. Med. Rep. 12 (5), 7293–7302. https://doi.org/10.3892/mmr.2015.4377.
Priftis, A., et al., 2017. MacroDevelopment of an assay to assess genotoxicity by particulate matter extract. Mol. Med. Rep. 15 (4), 1738–1746. https://doi.org/10.3892/mmr.2017.6171.
van Raamsdonk, J.M., Vega, I.E., Brundin, P., 2017. 'Oxidative stress in neurodegenerative disease: causation or association?'. Oncotarget 10777–10778. https://doi.org/10.18632/oncotarget.14650. Impact Journals LLC.
Radu, I.C., et al., 2019. Poly(3-hydroxybutyrate-CO-3-hydroxyvalerate) PHBHV biocompatible nanocarriers for 5-FU delivery targeting colorectal cancer. Drug Deliv. 26 (1), 318–327. https://doi.org/10.1080/10717544.2019.1582729.
Raman, V., et al., 2016. Synthesis of Co3O4 nanoparticles with block and sphere morphology, and investigation into the influence of morphology on biological toxicity. Experimental and Therapeutic Medicine 11 (2), 553–560. https://doi.org/10.3892/etm.2015.2946.
Ravi, M., et al., 2015. 3D cell culture systems: advantages and applications. J. Cell. Physiol. 230 (1), 16–26. https://doi.org/10.1002/jcp.24683.
Read, S.A.K., et al., 2014. Nanotechnology and exposure scenarios. In: Handbook of Nanosafety: Measurement, Exposure and Toxicology. Elsevier Inc., pp. 17–58. https://doi.org/10.1016/B978-0-12-416604-2.00002-0
Reddy, U.A., Prabhakar, P.V., Mahboob, M., 2017. Biomarkers of oxidative stress for in vivo assessment of toxicological effects of iron oxide nanoparticles. Saudi J. Biol. Sci. 24 (6), 1172–1180. https://doi.org/10.1016/j.sjbs.2015.09.029.
Reddy, Y.N., et al., 2004. Role of free radicals and antioxidants in tuberculosis patients. Indian J. Tubercul. 51 (4), 213–218.
Saifi, M.A., Khan, W., Godugu, C., 2018a. Cytotoxicity of nanomaterials: using nanotoxicology to address the safety concerns of nanoparticles. Pharm. Nanotechnol. 6 (1), 3–16. https://doi.org/10.2174/2211738505666171023152928.
Saifi, M.A., Khurana, A., Godugu, C., 2018b. Nanotoxicology: toxicity and risk assessment of nanomaterials. In: Nanomaterials in Chromatography: Current Trends in Chromatographic Research Technology and Techniques. Elsevier, pp. 437–465. https://doi.org/10.1016/B978-0-12-812792-6.00017-0.
Samadian, H., et al., 2020. Genotoxicity assessment of carbon-based nanomaterials; Have their unique physicochemical properties made them double-edged swords?. In: Mutation Research - Reviews in Mutation Research. Elsevier B.V., p. 108296. https://doi.org/10.1016/j.mrrev.2020.108296
Shangari, N., O'Brien, P.J., 2006. Catalase activity assays. Current Protocols in Toxicology 27 (1), 7.7.1–7.7.16. https://doi.org/10.1002/0471140856.tx0707s27.
Sharifi, S., et al., 2012. Toxicity of nanomaterials. Chem. Soc. Rev. 41 (6), 2323–2343. https://doi.org/10.1039/c1cs15188f.
Sharma, V., Kumar, A., Dhawan, A., 2012. Nanomaterials: exposure, effects and toxicity assessment. Proc. Natl. Acad. Sci. India B Biol. Sci. 82 (S1), 3–11. https://doi.org/10.1007/s40011-012-0072-7.
Sims, C.M., et al., 2017. Redox-active nanomaterials for nanomedicine applications. Nanoscale 15226–15251. https://doi.org/10.1039/c7nr05429g. Royal Society of Chemistry.
Smith, I.K., Vierheller, T.L., Thorne, C.A., 1988. 'Assay of glutathione reductase in crude tissue homogenates using 5,5′-dithiobis(2-nitrobenzoic acid)'. Anal. Biochem. 175 (2), 408–413. https://doi.org/10.1016/0003-2697(88)90564-7.
Smith, M.J., et al., 2016. Evaluating the Adverse Effects of Nanomaterials on the Immune System with Animal Models, pp. 281–315. https://doi.org/10.1142/9789813140431_0011.
Sochor, J., et al., 2012. Automation of methods for determination of lipid peroxidation. In: Lipid Peroxidation. InTech. https://doi.org/10.5772/45945.
Sosa, V., et al., 2013. 'Oxidative stress and cancer: an overview'. Ageing Res. Rev. 376–390. https://doi.org/10.1016/j.arr.2012.10.004. Elsevier.
Soumya, R., Vani, R., 2015. 'CUPRAC–BCS and antioxidant activity assays as reliable markers of antioxidant capacity in erythrocytes'. Hematology 20 (3), 165–174. https://doi.org/10.1179/1607845414Y.0000000177.
Stagos, D., et al., 2014. Antiangiogenic potential of grape stem extract through inhibition of vascular endothelial growth factor expression. J. Physiol. Pharmacol. 65 (6), 843–852. Available at: https://europepmc.org/article/med/25554988. (Accessed 3 January 2021).
Stagos, D., et al., 2018. Extracts from the mediterranean food plants Carthamus lanatus, Cichorium intybus, and Cichorium spinosum enhanced GSH levels and increased Nrf2 expression in human endothelial cells. Oxidative Medicine and Cellular Longevity. https://doi.org/10.1155/2018/6594101, 2018.
Staroń, A., et al., 2020. Analysis of the exposure of organisms to the action of nanomaterials. Materials 13 (2), 349. https://doi.org/10.3390/ma13020349.
Strober, W., 2015. Trypan blue exclusion test of cell viability. Curr. Protoc. Im. 111 (1), A3.B.1–A3.B.3. https://doi.org/10.1002/0471142735.ima03bs111.
Sukhanova, A., et al., 2018. 'Dependence of nanoparticle toxicity on their physical and chemical properties'. Nanoscale Research Letters. https://doi.org/10.1186/s11671-018-2457-x. Springer New York LLC.
Taghizadehghalehjoughi, A., et al., 2018. Effect of metformin/irinotecan-loaded poly-lactic-co-glycolic acid nanoparticles on glioblastoma: in vitro and in vivo studies. Nanomedicine 13 (13), 1595–1606. https://doi.org/10.2217/nnm-2017-0386.
Tekos, F., et al., 2020. The importance of redox status in the frame of lifestyle approaches and the genetics of the lung innate immune molecules, SP-A1 and SP-A2, on differential outcomes of covid-19 infection. Antioxidants 9 (9), 1–22. https://doi.org/10.3390/antiox9090784.
Thomas, T., et al., 2009. Moving toward exposure and risk evaluation of nanomaterials: challenges and future directions. Wiley Interdisciplinary Reviews: Nanomedicine and Nanobiotechnology 1 (4), 426–433. https://doi.org/10.1002/wnan.34.
Tsatsakis, A.M., et al., 2017. Simulating real-life exposures to uncover possible risks to human health: a proposed consensus for a novel methodological approach. Hum. Exp. Toxicol. 36 (6), 554–564. https://doi.org/10.1177/0960327116681652.
Tsatsakis, A.M., Docea, A.O., Tsitsimpikou, C., 2016. 'New challenges in risk assessment of chemicals when simulating real exposure scenarios; simultaneous multi-chemicals' low dose exposure'. Food Chem. Toxicol. 96, 174–176. https://doi.org/10.1016/j.fct.2016.08.011.
Tsiaoussis, J., et al., 2019. Effects of single and combined toxic exposures on the gut microbiome: current knowledge and future directions. Toxicol. Lett. 312, 72–97. https://doi.org/10.1016/j.toxlet.2019.04.014.
Turan, N.B., et al., 2019. 'Nanoparticles in the aquatic environment: usage, properties, transformation and toxicity—a review'. Process Saf. Environ. Protect. 238–249. https://doi.org/10.1016/j.psep.2019.08.014. Institution of Chemical Engineers.
Valgimigli, L., Baschieri, A., Amorati, R., 2018. Antioxidant activity of nanomaterials. J. Mater. Chem. B 2036–2051. https://doi.org/10.1039/c8tb00107c. Royal Society of Chemistry.
Veskoukis, A., et al., 2019. A battery of translational biomarkers for the assessment of the in vitro and in vivo antioxidant action of plant polyphenolic compounds: the biomarker issue. Current Opinion in Toxicology 99–109. https://doi.org/10.1016/j.cotox.2018.10.001. Elsevier B.V.
Veskoukis, A.S., et al., 2009. Blood reflects tissue oxidative stress depending on biomarker and tissue studied. Free Radic. Biol. Med. 47 (10), 1371–1374. https://doi.org/10.1016/j.freeradbiomed.2009.07.014.
Veskoukis, A.S., et al., 2016. 'Spectrophotometric assays for measuring redox biomarkers in blood'. Biomarkers 208–217. https://doi.org/10.3109/1354750X.2015.1126648. Taylor and Francis Ltd.
Veskoukis, A.S., Tsatsakis, A., Kouretas, D., 2020. Approaching reactive species in the frame of their clinical significance: a toxicological appraisal. Food Chem. Toxicol. https://doi.org/10.1016/j.fct.2020.111206. Elsevier Ltd.
Viswanath, B., Kim, S., 2017. Influence of nanotoxicity on human health and environment: the alternative strategies. Rev. Environ. Contam. Toxicol. 242 https://doi.org/10.1007/398_2016_12.
Wang, S., Yu, H., Wickliffe, J.K., 2011. Limitation of the MTT and XTT assays for measuring cell viability due to superoxide formation induced by nano-scale TiO 2. Toxicol. Vitro 25 (8), 2147–2151. https://doi.org/10.1016/j.tiv.2011.07.007.
Watkinson, A.C., et al., 2013. Nanoparticles do not penetrate human skin - a theoretical perspective. Pharmaceutical Research. Pharm Res 1943–1946. https://doi.org/10.1007/s11095-013-1073-9.
Wilhelmi de Toledo, F., et al., 2020. Influence of long-term fasting on blood redox status in humans. Antioxidants 9 (6), 496. https://doi.org/10.3390/antiox9060496.
Woodruff, R.S., et al., 2012. Genotoxicity evaluation of titanium dioxide nanoparticles using the Ames test and Comet assay. J. Appl. Toxicol. 32 (11), 934–943. https://doi.org/10.1002/jat.2781.
Wörle-Knirsch, J.M., Pulskamp, K., Krug, H.F., 2006. Oops they did it again! Carbon nanotubes hoax scientists in viability assays. Nano Lett. 6 (6), 1261–1268. https://doi.org/10.1021/nl060177c.
Wu, W. Te, et al., 2019. Longitudinal follow-up of health effects among workers handling engineered nanomaterials: a panel study. Environ. Health: A Global Access Science Source 18 (1), 107. https://doi.org/10.1186/s12940-019-0542-y.
Wu, Z., et al., 2017. Assessment of the toxicity and inflammatory effects of different-sized zinc oxide nanoparticles in 2D and 3D cell cultures. RSC Adv. 7 (21), 12437–12445. https://doi.org/10.1039/c6ra27334c.
Xiarchos, I., et al., 2020. Nanocharacterization, materials modeling, and research integrity as enablers of sound risk assessment: designing responsible nanotechnology. Small 16 (36), 2001590. https://doi.org/10.1002/smll.202001590.
Yen, G.C., Duh, P. Der, 1993. Antioxidative properties of methanolic extracts from peanut hulls. JAOCS (J. Am. Oil Chem. Soc.) 70 (4), 383–386. https://doi.org/10.1007/BF02552711.
Yi, J., et al., 2013. Whole-body nanoparticle aerosol inhalation exposures. JoVE (75). https://doi.org/10.3791/50263.
Yoshida, R., Kitamura, D., Maenosono, S., 2009. Mutagenicity of water-soluble ZnO nanoparticles in Ames test. J. Toxicol. Sci. 34 (1), 119–122. https://doi.org/10.2131/jts.34.119.
Zamboni, W.C., et al., 2018. 'Animal models for analysis of immunological responses to nanomaterials: challenges and considerations'. Adv. Drug Deliv. Rev. 82–96. https://doi.org/10.1016/j.addr.2018.09.012. Elsevier B.V.
Zare, M., et al., 2018. Surfactant assisted solvothermal synthesis of ZnO nanoparticles and study of their antimicrobial and antioxidant properties. J. Mater. Sci. Technol. 34 (6), 1035–1043. https://doi.org/10.1016/j.jmst.2017.09.014.
Zeiger, E., 2019. 'The test that changed the world: the Ames test and the regulation of chemicals'. Mutat. Res. Genet. Toxicol. Environ. Mutagen 43–48. https://doi.org/10.1016/j.mrgentox.2019.05.007. Elsevier B.V.